Cancer Cell

Article

The crosstalk between macrophages and cancer cells potentiates pancreatic cancer cachexia

Graphical abstract

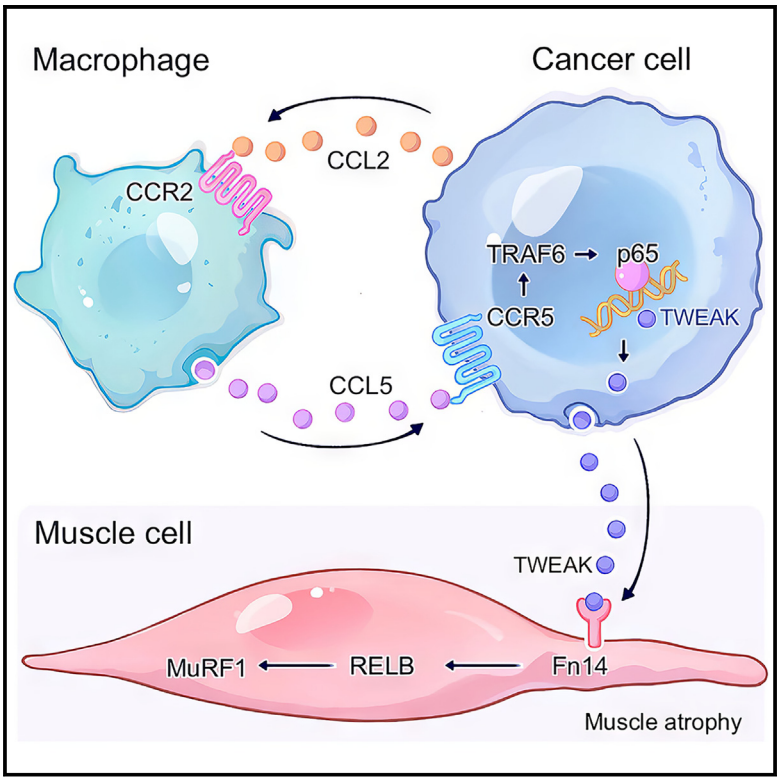

Highlights

- Macrophages facilitate pancreatic cancer derived TWEAK to induce muscle wasting
- CCL5 promotes pancreatic cancer cachexia through p65 mediated TWEAK upregulation
- CCL2 activates macrophages to induce non-autonomous activation of TWEAK in tumor

Authors

Mingyang Liu, Yu Ren, Zhijun Zhou, ..., Courtney W. Houchen, Yuqing Zhang, Min Li

Correspondence

Yuqing-Zhang@ouhsc.edu (Y.Z.), Min-Li@ouhsc.edu (M.L.)

In brief

Liu et al. identify a novel feedforward loop between tumor cells and macrophages that promotes muscle wasting. Specifically, tumor-derived CCL2 activates macrophages to facilitate non-autonomous activation of TWEAK in tumor cells via CCL5/p65 signaling, leading to cachexia. Macrophage depletion and TWEAK inhibition represent promising therapeutic targets for pancreatic cancer cachexia.

Liu et al., 2024, Cancer Cell *42*, 885–903
May 13, 2024
https://doi.org/10.1016/j.ccell.2024.03.009

CellPress

Cancer Cell

CellPress
OPEN ACCESS

Article

The crosstalk between macrophages and cancer cells potentiates pancreatic cancer cachexia

Mingyang Liu,[1,2,8] Yu Ren,[1,2,8] Zhijun Zhou,[1,2,8] Jingxuan Yang,[1,2,8] Xiuhui Shi,[1,2,8] Yang Cai,[1,2,8] Alex X. Arreola,[1,3] Wenyi Luo,[4] Kar-Ming Fung,[3] Chao Xu,[5] Ryan D. Nipp,[1] Michael S. Bronze,[1] Lei Zheng,[6] Yi-Ping Li,[7] Courtney W. Houchen,[1] Yuqing Zhang,[1,2,*] and Min Li[1,2,9,*]

[1]Department of Medicine, The University of Oklahoma Health Sciences Center, Oklahoma City, OK 73104, USA
[2]Department of Surgery, The University of Oklahoma Health Sciences Center, Oklahoma City, OK 73104, USA
[3]Department of Pathology, The University of Oklahoma Health Sciences Center, Oklahoma City, OK 73104, USA
[4]Department of Pathology, Yale School of Medicine, New Haven, CT 06519, USA
[5]Department of Biostatistics and Epidemiology, Hudson College of Public Health, The University of Oklahoma Health Sciences Center, Oklahoma City, OK 73104, USA
[6]Sidney Kimmel Comprehensive Cancer Center, Johns Hopkins University School of Medicine, Baltimore, MD 21287, USA
[7]Department of Integrative Biology & Pharmacology, The University of Texas Health Science Center at Houston, Houston, TX 77030, USA
[8]These authors contributed equally
[9]Lead contact
*Correspondence: Yuqing-Zhang@ouhsc.edu (Y.Z.), Min-Li@ouhsc.edu (M.L.)
https://doi.org/10.1016/j.ccell.2024.03.009

SUMMARY

With limited treatment options, cachexia remains a major challenge for patients with cancer. Characterizing the interplay between tumor cells and the immune microenvironment may help identify potential therapeutic targets for cancer cachexia. Herein, we investigate the critical role of macrophages in potentiating pancreatic cancer induced muscle wasting via promoting TWEAK (TNF-like weak inducer of apoptosis) secretion from the tumor. Specifically, depletion of macrophages reverses muscle degradation induced by tumor cells. Macrophages induce non-autonomous secretion of TWEAK through CCL5/TRAF6/NF-κB pathway. TWEAK promotes muscle atrophy by activating MuRF1 initiated muscle remodeling. Notably, tumor cells recruit and reprogram macrophages via the CCL2/CCR2 axis and disrupting the interplay between macrophages and tumor cells attenuates muscle wasting. Collectively, this study identifies a feedforward loop between pancreatic cancer cells and macrophages, underlying the non-autonomous activation of TWEAK secretion from tumor cells thereby providing promising therapeutic targets for pancreatic cancer cachexia.

INTRODUCTION

Pancreatic cancer currently represents the third leading cause of cancer-associated death in the United States, with projections suggesting this malignancy may become the second leading cause of cancer death within this decade.[1,2] Over 80% of patients with pancreatic cancer present with advanced-stage tumors at diagnosis, when curative treatment options are limited.[3] Most of these patients develop cancer cachexia, a debilitating syndrome characterized by uncontrollable body weight loss, lack of appetite, and muscle wasting.[4–6] Unfortunately, no approved therapies for cancer cachexia exist in the United States.[7] Therefore, there is a pressing need to identify potential therapeutic targets and develop effective treatment options for cancer cachexia.

Tumor immune microenvironment plays an important role in cancer progression and cachexia.[8–10] Macrophages represent one of the most abundant immune cell types in pancreatic cancer immune microenvironment and are associated with cancer progression and metastasis.[11,12] Emerging evidence suggests that macrophages play key roles in both muscle wasting and muscle regeneration,[13] and CCL2/MCP1 is a central cytokine in regulating the infiltration and polarization of monocytes/macrophages.[14,15] In patients with pancreatic cancer experiencing cachexia, research has demonstrated increased levels of CCL2 in serum.[16] However, the function and underlying mechanism of the crosstalk between cancer cells and macrophages in cancer cachexia remains undefined.

Inflammation represents one of the key hallmarks of cancer cachexia.[17] Cancer cells induce systemic inflammation by secreting soluble factors (i.e., cytokines, chemokines, and hormones) as well as extracellular vesicles and particles (EVPs).[18] Studies have identified several inflammatory cytokines as regulators for muscle wasting in pancreatic cancer, such as IL-1, IL-6, IL-8, and TNF-α.[19–21] In prior work, we found that pancreatic cancer promotes muscle wasting through the secretion of

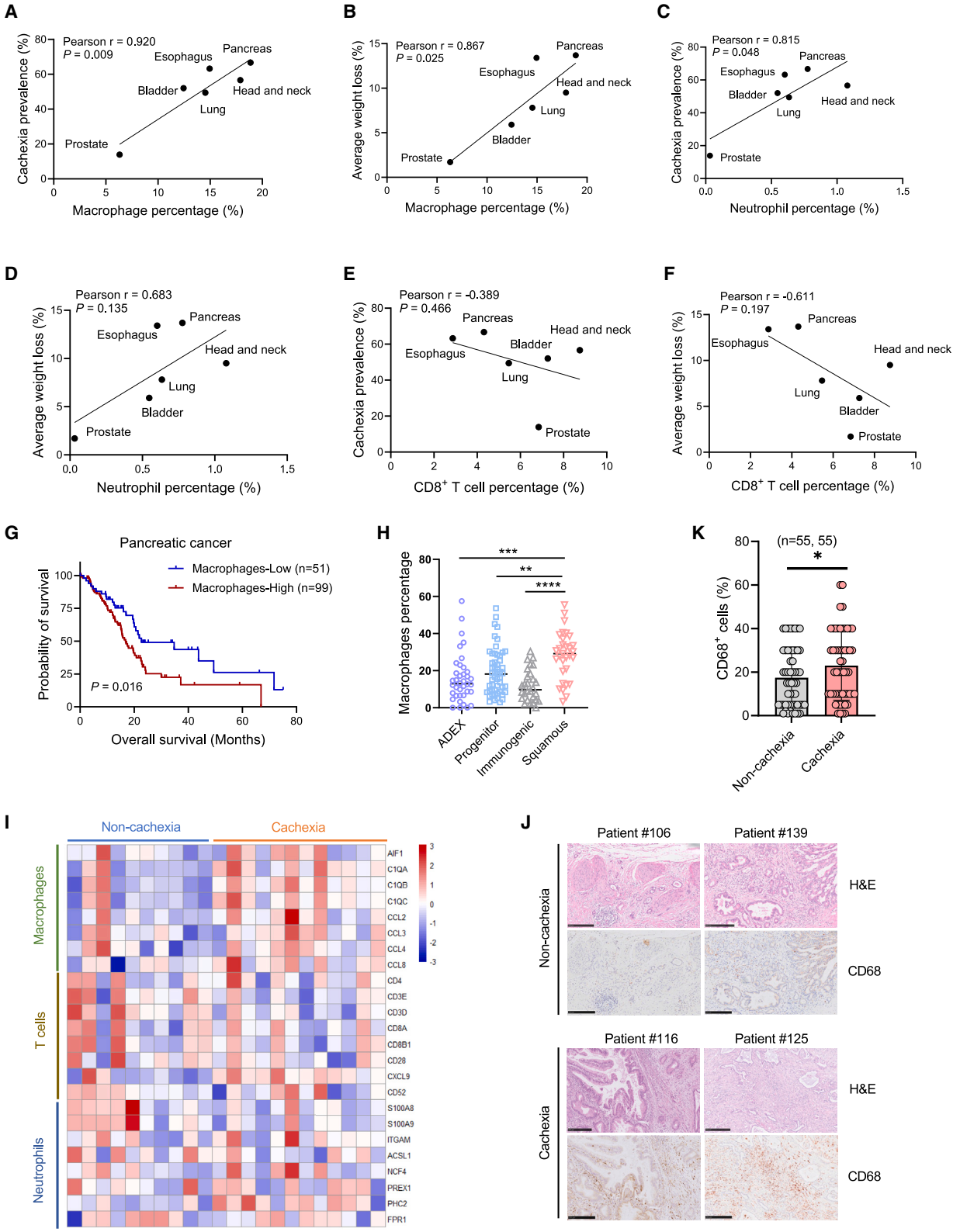

Figure 1. Tumor-associated macrophages promote muscle wasting and cancer cachexia

(A–F) Analysis of the correlation between cancer cachexia prevalence, body weight loss with the percentage of immune cells (macrophages, neutrophils, and CD8$^+$ T cells) in tumor tissue of several cancer types (n = 6) in TCGA database. Statistical analysis by Pearson's correlation test.

(legend continued on next page)

TGF-β, TNFSF10, and extracellular vesicles containing Hsp70/90.[22–24] Additionally, inflammatory cytokines secreted from the tumor microenvironment also facilitate cancer cachexia and cancer progression.[25,26] Despite extensive work correlating inflammatory cytokines with cancer cachexia, the mechanism of tumor microenvironment regulation of tumor derived muscle wasting factors remains elusive.

In the current study, we sought to identify associations among the infiltration of macrophages with cachexia in pancreatic cancer. Specifically, we aimed to characterize macrophage recruitment by tumor cells via CCL2/CCR2 axis, which promotes muscle wasting in pancreatic cancer. In addition, we further explored the role of macrophages in facilitating cancer cell-derived TWEAK (TNF-like weak inducer of apoptosis) secretion, which may contribute to CCL2-driven muscle wasting. By identifying a potential mechanism of crosstalk between pancreatic cancer cells and macrophages, this work could aid in shaping future therapeutic development targeting muscle wasting in pancreatic cancer patients suffering from cachexia.

RESULTS

Macrophages promote muscle wasting and cancer cachexia

In order to investigate the crosstalk between immune cells and cancer cachexia, we analyzed the correlation between different types of immune cells and cancer cachexia in several cancer types.[4,27] Since there are very limited datasets that provide the information of both cachexia and immune cells in tumor tissues, we analyzed multiple datasets, aiming to elucidate the potential link between immune cells and cancer cachexia. We found that macrophages are the most abundant immune cells and positively associated with cancer cachexia prevalence and body weight loss (Figures 1A–1F and S1A). Single-cell sequencing analysis of the GSE154778 dataset showed that late-stage pancreatic cancer tissue had higher macrophage infiltration compared to that in early stage tumors (Figure S1B). Macrophage infiltration was associated with worse overall survival in pancreatic cancer (Figure 1G). We further analyzed the correlation between macrophage infiltration and different molecular subtypes of pancreatic cancer and demonstrated the highest macrophage infiltration rate in squamous subtype, which is associated with the worst prognosis among all subtypes (Figure 1H). The signature for tumor-associated macrophages (TAMs) was enriched in progressive cancers and associated with poor prognosis.[28] We then validated these findings in an independent cohort by analyzing the expression of signature genes of TAMs, T cells, and neutrophils and found that cachectic cancer types (pancreatic cancer, esophagus cancer, head and neck cancer, and lung cancer) displayed enrichment of the TAM signature genes compared to that in less-cachectic cancer types (prostate cancer) (Figure S1C). We further examined the enrichment of immune signature genes in a cancer cachexia dataset.[29] We found that the TAM signature was enriched in tumor tissue of cachectic mice compared to non-cachectic mice (Figure 1I). We further validated these findings in a cohort of pancreatic cancer patients and found that the percentage of CD68 (macrophage marker) positive cells in human pancreatic cancer tissues was higher in individuals with cachexia compared to those without cachexia (Figures 1J and 1K). Macrophage percentage in tumor tissue is also positively correlated with body weight loss percentage in patients with pancreatic cancer (Figure S1D). Collectively, these data indicated that macrophages may play a pivotal role in pancreatic cancer cachexia.

Depletion of macrophages attenuates muscle atrophy in pancreatic cancer mouse models

To further determine the role of macrophages in pancreatic cancer cachexia, we established the macrophage-depleted mouse models, including the *Ccr2*$^{-/-}$ mouse model and clodronate treatment model.[30,31] We established the KPC orthotopic allograft mouse model in C57BL/6 WT and *Ccr2*$^{-/-}$ mice. Tumor growth between WT and *Ccr2*$^{-/-}$ mice bearing the KPC tumors are comparable (Figures 2A and S2A). *Ccr2*$^{-/-}$ mice showed significant reduction of CCR2^{+} macrophages in the tumor and spleen tissues compared to that in the WT mice (Figures 2B, 2C, and S2B). There was no significant difference of basal muscle status between C57BL/6 WT and *Ccr2*$^{-/-}$ mice without tumor engraftment (Figures S2C–S2G). Intriguingly, we found increased grip strength in *Ccr2*$^{-/-}$ mice compared to WT mice with orthotopic allograft of KPC tumors (Figure 2D). Moreover, *Ccr2*$^{-/-}$ mice showed attenuated body weight loss compared to WT mice (Figure S2H). We further evaluated tibialis anterior (TA) and gastrocnemius (GAS) muscle weight in mice bearing tumors. *Ccr2*$^{-/-}$ mice had higher TA muscle and GAS muscle weight compared to WT mice (Figures 2E, S2I, and S2J). Analysis of cross-sectional areas of muscle fiber also indicated that *Ccr2*$^{-/-}$ mice attenuated tumor-induced muscle wasting (Figure 2F). Furthermore, we examined the expression of muscle wasting markers MuRF1 and Atrogin-1 in TA muscle tissues of WT or *Ccr2*$^{-/-}$ mice. We found that *Ccr2*$^{-/-}$ mice had lower expression of muscle wasting markers in TA muscle (Figure 2G). These findings demonstrated that depletion of macrophages by *Ccr2* knockout attenuated tumor-induced muscle wasting. To further validate these findings, we established another macrophage-depleted mouse model via clodronate treatment, which pharmacologically depleted macrophages (Figures 2H, 2I, and S2K). The basal muscle levels were comparable between PBS or clodronate treatment groups without tumor engraftment (Figures S2L–S2P), while clodronate treatment increased the

(G) Survival analysis of pancreatic cancer patients with macrophage-low or macrophage-high tumors in TCGA database. Statistical analysis by Log rank test. n = 51, 99/group.

(H) Analysis of the correlation between molecular subtypes of pancreatic cancer and macrophage percentage in tumor tissue. Horizon line indicates median value. n = 38, 53, 28, 31/group. **, $p < 0.01$; ***, $p < 0.001$; ****, $p < 0.0001$ by *t* test.

(I) The levels of immune-cell associated signature genes in the tumor tissue of non-cachexia and lung cancer cachexia mouse model using the GSE165856 dataset.

(J) Representative images of H&E staining and IHC staining of CD68 in pancreatic cancer patients with/without cachexia. The scale bars represent 250 μm.

(K) Statistical analysis of experiments in (J). n = 55/group; mean ± SD. *, $p < 0.05$ by Mann-Whitney test. See also Figure S1.

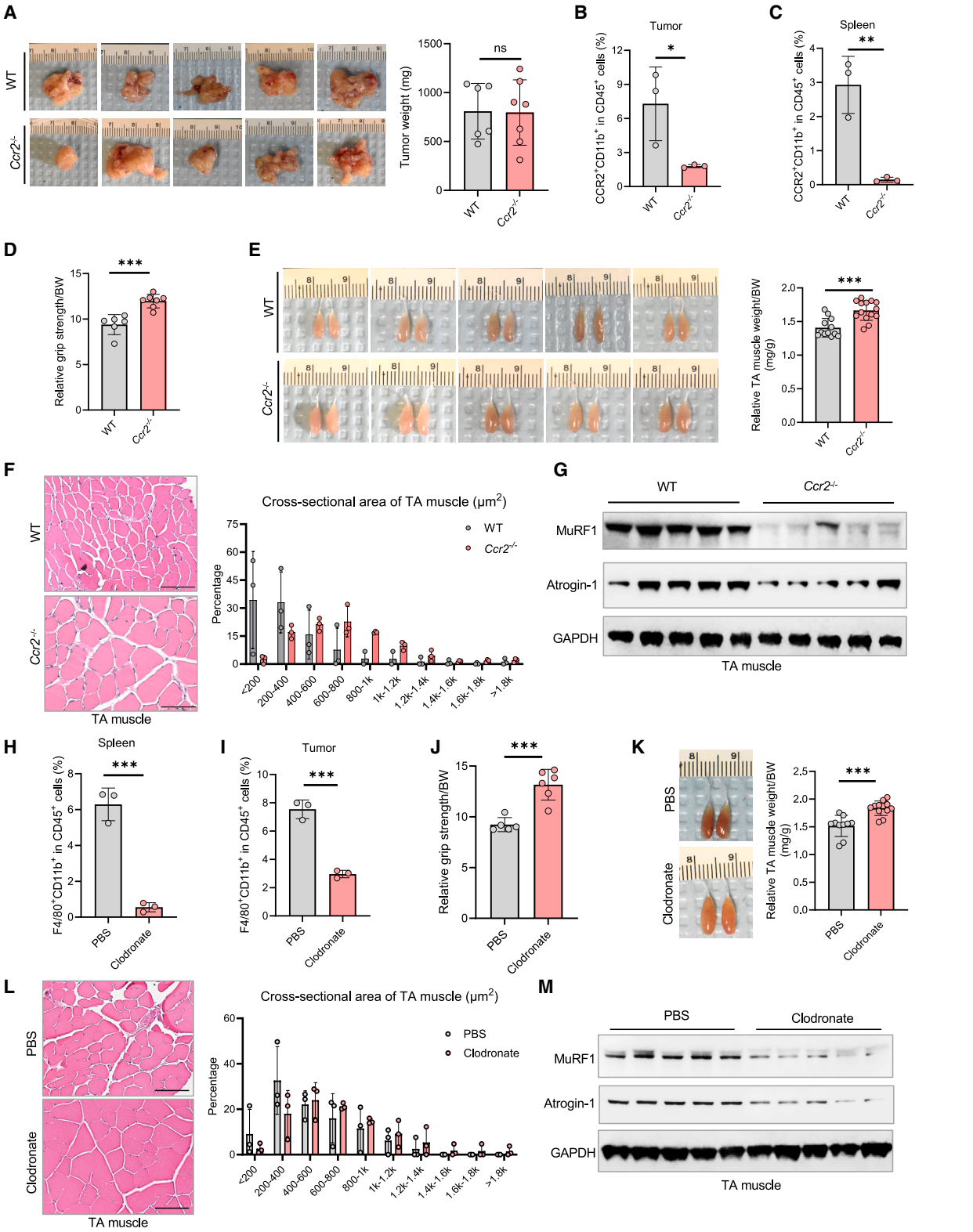

Figure 2. Depletion of macrophages attenuates muscle atrophy in pancreatic cancer mouse models

(A) Representative tumor tissue and tumor weight of WT and *Ccr2*$^{-/-}$ mice bearing allograft tumor from KPC cells. n = 6, 7/group; mean ± SD; ns, not significant by t test.

(B and C) The levels of CCR2^{+} macrophages in the spleen and tumor tissue of WT and *Ccr2*$^{-/-}$ mice. n = 3/group; mean ± SD; *, $p < 0.05$; **, $p < 0.01$ by t test.

(legend continued on next page)

grip strength of mice with tumors (Figure 2J). Clodronate treatment also suppressed muscle atrophy and tumor growth compared to mice receiving PBS-liposome treatment (Figures 2K, 2L, S2Q, and S2R). The expression of muscle wasting markers decreased in clodronate treatment group (Figure 2M). These results indicated that macrophages promote tumor-induced muscle atrophy in mouse models.

Macrophages promote muscle wasting by upregulating TWEAK in pancreatic cancer

TWEAK, also known as TNFSF12, is a member of the TNF superfamily.[32] Our previous studies indicated that TRAIL (TNF-related apoptosis-inducing ligand) (TNFSF10) promotes muscle wasting in pancreatic cancer.[24] However, the role of TWEAK in pancreatic cancer muscle wasting remains elusive. We found that TWEAK expression was positively associated with M2 but not M0 or M1 macrophages infiltration in human pancreatic cancer tissues in the TCGA dataset (Figures 3A, S3A and S3B). The mRNA levels of *Il10*, *Tgfb1*, and *Arg1* were significantly increased in macrophages when co-cultured with pancreatic cancer cells (Figures S3C–S3F). TWEAK recombinant protein increased the expression of muscle wasting markers Atrogin-1 and MuRF1 as well as RELB signaling pathway in C2C12 differentiated myotubes (Figures 3B and S3G). We noticed that TWEAK expression in orthotopic KPC tumor tissues was higher than that in normal pancreas from the sham group (Figure 3C). In spontaneous pancreatic cancer models (*LSL-Kras*$^{G12D/+}$; *LSL-Trp53*$^{R172H/+}$; *Pdx1-Cre*), the expression of TWEAK increased as tumor progressed (Figures 3D and S3H). Indeed, the endogenous level of TWEAK was extremely low in pancreatic cancer cell lines (Figure 3E). However, when co-cultured with macrophages, the secretion level of mTWEAK was significantly increased in pancreatic cancer cells, indicating that TWEAK may be upregulated in a non-autonomous manner (Figure 3E). Consistently, the conditioned medium from macrophages treated with IL-4 and IL-10 increased the secretion of TWEAK in KPC and AsPC-1 cells (Figures S3I and S3J). Immunofluorescence staining of TWEAK, CD68, and pan-CK in the tumor tissue of mice bearing CAC tumors showed the co-localization signal between TWEAK and pan-CK, but not with CD68, indicating that TWEAK is mainly from tumor cells (Figure 3F). We further examined TWEAK expression in pancreatic cancer cells and found consistent results to that of ELISA (Figures 3G and S3K). Patient-derived primary human pancreatic cancer cells (PDX46 and PDX87) were utilized to validate the role of macrophages in promoting muscle wasting.[33] The expression of TWEAK in PDX46 and PDX87 cells was increased when these cells were co-cultured with macrophages (Figures 3H and S3L). TWEAK expression was increased in KPC and AsPC-1 cells when treated with the conditioned medium derived from CCL2-activated macrophages (Figure 3I). CCL2 itself did not affect TWEAK expression in either KPC or AsPC-1 cells (Figure S3M). Knockdown of TWEAK in tumor cells reversed the pro-cachexia effects induced by macrophages (Figures 3J, S3N, and S3O). The expression of muscle wasting markers in C2C12-derived myotubes increased when the myotubes were treated with conditioned medium from PDX46 and PDX87 cells co-cultured with macrophages, indicating that macrophages increase the pro-cachexia potential of these patient-derived primary pancreatic cancer cells (Figure 3K). TWEAK expression decreased in the tumor tissue of *Ccr2*$^{-/-}$ transgenic mice bearing KPC tumors, compared to that of C57BL/6 WT mice (Figure 3L). These findings indicated that macrophages facilitated tumor-derived TWEAK secretion to upregulate the expression of muscle atrophy markers.

Macrophage-derived CCL5 upregulates TWEAK via p65 signaling to promote pancreatic cancer cachexia

Chemokines are key mediators of cancer progression and cancer cachexia.[16,25,32] To uncover the mechanism of macrophages promoting tumor-derived TWEAK, we examined the mRNA levels of several cytokines in macrophages through non-contacted co-culture with pancreatic cancer cells. C-C motif chemokine ligand 5 (CCL5) was significantly upregulated in macrophages when co-cultured with KPC and AsPC-1 cells (Figures 4A and S4A). Similar results were found in macrophages directly cultured with pancreatic cancer cells (Figures S4B and S4C). The conditioned medium from AsPC-1 cells also increased mRNA levels of *Ccl5* in macrophages (Figure S4D). Meanwhile, macrophages co-cultured with pancreatic cancer cells showed increased CCL5 secretion (Figures 4B and 4C). Treatment with recombinant protein CCL5 increased mRNA, protein, as well as secretion of TWEAK in both KPC and AsPC-1 cells (Figures 4D, 4E, S4E, and S4F). CCL5 alone did not induce muscle wasting of C2C12 myotubes. However, the conditioned medium from cancer cells treated with CCL5 induced MuRF1 and Atrogin-1 expression in C2C12 myotubes (Figures 4F and 4G).

(D) Relative grip strength of mice from experiment shown in (A). n = 6, 7/group; mean ± SD; ***, $p < 0.001$ by t test.
(E) Representative images of TA muscle from mice shown in (A). Right, relative muscle weight to body weight (BW). n = 12, 14/group; mean ± SD; ***, $p < 0.001$ by t test.
(F) Representative images of H&E staining of TA muscle sections of WT and *Ccr2*$^{-/-}$ transgenic mice bearing allograft tumor from KPC cells. Scale bar represents 50 μm. Right, quantitative analysis of cross-sectional areas of muscle fibers. Mean ± SD.
(G) Expression levels of muscle wasting protein MuRF1 and Atrogin-1 were detected in TA muscle tissue from WT or *Ccr2*$^{-/-}$ transgenic mice bearing allograft tumor from KPC cells.
(H and I) The levels of F4/80^{+} macrophages in the spleen and tumor tissue of mice treated with PBS or clodronate.
n = 3/group; mean ± SD; ***, $p < 0.001$ by t test.
(J) Relative grip strength of WT mice bearing tumors from KPC cells and treated with PBS or clodronate. n = 5, 6/group; mean ± SD; ***, $p < 0.001$ by t test.
(K) Representative images of TA muscle from WT mice bearing tumors from KPC cells and treated with PBS or clodronate. Right, relative muscle weight to BW. n = 10, 12/group; mean ± SD; ***, $p < 0.001$ by t test.
(L) Representative images of H&E staining of TA muscle sections of WT mice bearing allograft tumor from KPC cells and treated with PBS or clodronate. Scale bar represents 50 μm.
(M) Expression levels of muscle wasting protein MuRF1 and Atrogin-1 were detected in TA muscle tissue from WT mice bearing allograft tumor from KPC cells and treated with PBS or clodronate. See also Figure S2.

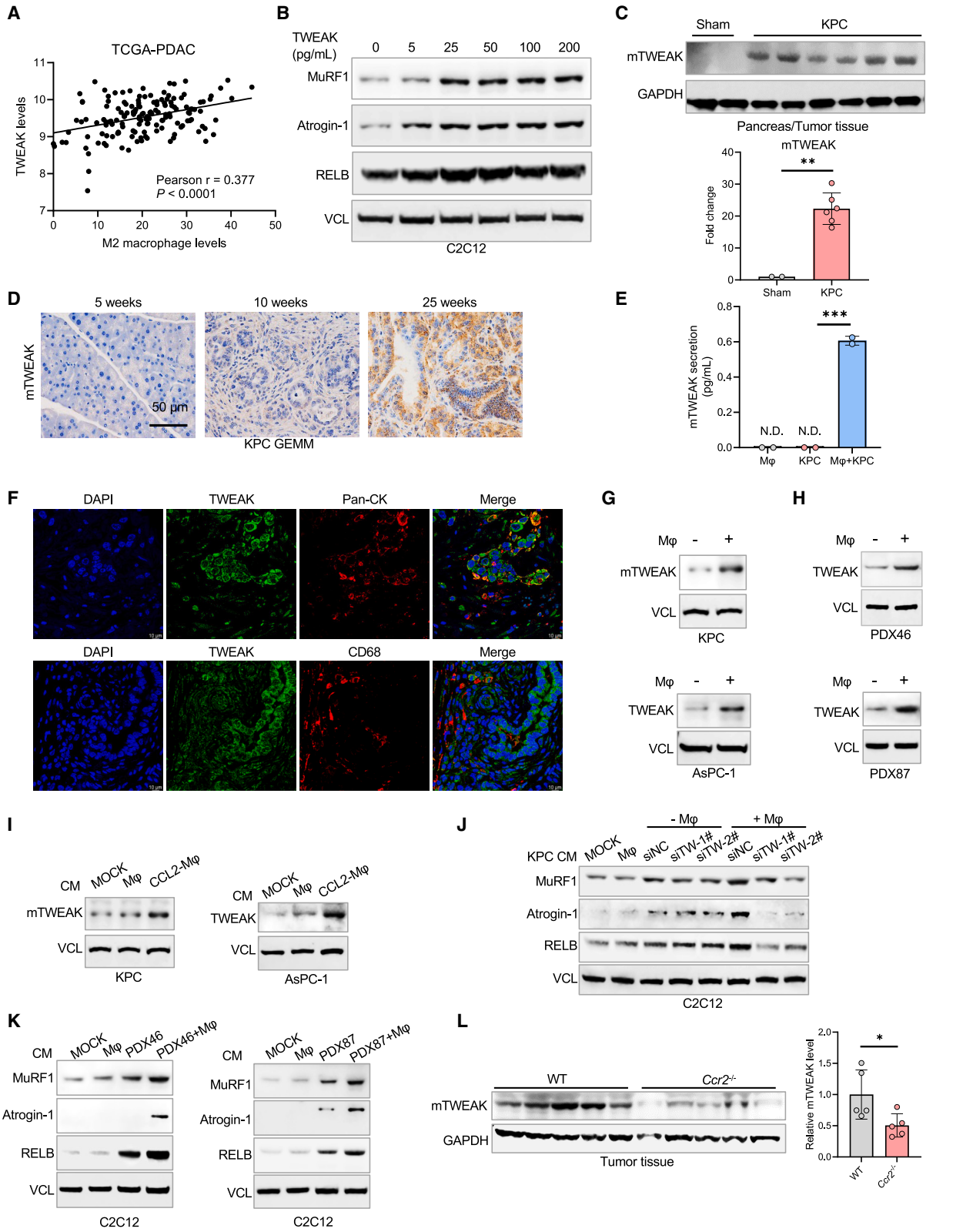

Figure 3. Macrophages promote muscle wasting by upregulating TWEAK in pancreatic cancer

(A) The correlation of M2 macrophages infiltration and TWEAK expression in pancreatic cancer tissue in TCGA database (n = 150). Statistical analysis by Pearson's correlation test.

(legend continued on next page)

We further examined whether CCL5 regulates TWEAK expression in pancreatic cancer cells. To demonstrate that macrophage-induced TWEAK expression in pancreatic cancer cells is dependent on CCL5/CCR5 signaling axis, we knocked down CCR5 in tumor cells and found that inhibition of CCL5/CCR5 pathway would reverse macrophage-induced TWEAK upregulation (Figures 4H and 4I). Furthermore, inhibition of CCL5/CCR5 pathway results in the decrease of muscle wasting markers induced by tumor and macrophages crosstalk (Figures 4J and 4K). To investigate the mechanism through which CCL5 upregulates TWEAK expression, we examined the potential signaling pathways. NF-κB pathway (p65) was reported to be the downstream target of CCL5, which also plays critical roles in cancer cachexia.[34,35] The results of chromatin immunoprecipitation (ChIP) assay and luciferase assay confirmed that p65 transcriptionally activates TWEAK (Figures 4L and 4M). In addition, p65 (also known as RELA) is associated with TWEAK expression in human pancreatic cancer tissues in TCGA database (Figure S4G). Moreover, inhibition of p65 pathway by small molecule inhibitor QNZ (EVP4593) blocked macrophage-induced TWEAK expression in AsPC-1 cells, indicating that NF-κB signaling is required for macrophage-promoted cancer-derived TWEAK expression (Figures 4N and S4H–S4K). High level of CCL5 in pancreatic cancer tissue was associated with worse prognosis (Figure S4L). Thus, these results suggested that CCL5 facilitates cancer cell-derived TWEAK secretion by activating the NF-κB axis (p65).

Pancreatic cancer cells recruit macrophages, which induce non-autonomous activation of TWEAK via TRAF6/p65 pathway

To further explore the underlying mechanism of CCL5-induced TWEAK expression, we established two variants of KPC and AsPC-1 cell lines with different cachectic potential: one with high cachectic potential (named "CAC") and the other one with relatively low cachectic potential (named "non-CAC") based on the expression of muscle wasting biomarkers, such as Atrogin-1 and MuRF1 in muscle tissue. KPC-CAC tumors induced more severe muscle wasting compared to non-CAC tumors (Figures S5A and S5B). KPC-CAC tumor tissue showed increased infiltration of macrophages compared to that in KPC-non-CAC tumors (Figures 5A and S5C). Meanwhile, the KPC-CAC tumors had higher mRNA levels of *Ccl5* (Figure 5B). Consistently, we found higher expression of CCL5 in CAC tumors compared to non-CAC tumors in WT mice. When the tumors were allografted on *Ccr2*$^{-/-}$ transgenic mice, CCL5 levels in CAC tumors and non-CAC tumors were comparable (Figure 5C). Non-CAC tumors showed lower mRNA levels of *Tnfsf12* which encodes TWEAK (Figure 5D). We also evaluated TWEAK levels in mouse serum by ELISA and found that mice allografted with CAC tumors had higher levels of TWEAK compared to that with non-CAC tumors (Figure 5E). CCL5 induced TWEAK expression in CAC cell lines but not in non-CAC cell lines (Figures 5F and 5G). These findings suggest that CAC tumor facilitates the recruitment of macrophages. Reciprocally, CCL5 secretion from macrophages promotes the secretion of TWEAK from cancer cells, forming a feedforward loop.

Next, we explored the underlying mechanism of CCL5-induced activation of NF-κB signaling in cancer cells. Emerging evidence indicated that TRAF6 plays an essential role in skeletal muscle mass regulation and serves as a pivotal regulator of canonical NF-κB.[36] We found that protein levels of TRAF6 in pancreatic cancer cells increased when co-cultured with macrophages (Figures 5H and 5I). Tumor tissue of mice bearing allograft from CAC cells showed higher TRAF6 and nuclear p65 expression compared to that of non-CAC cells (Figure S5D). Consistently, conditioned medium from M2 macrophages activated TRAF6/NF-κB signaling in CAC-but not in non-CAC (Figures 5J and S5E). Then, we used recombinant protein CCL5 to treat KPC and AsPC-1 cells and found that TRAF6 was upregulated in CAC but not in non-CAC (Figures 5K and 5L). Meanwhile, the conditioned medium from KPC cells treated with CCL5 upregulated MuRF1 and Atrogin-1 in C2C12 differentiated myotubes (Figure S5F). To examine whether TRAF6 is involved in macrophage-induced TWEAK expression, we overexpressed TRAF6 in both CAC and non-CAC cells and found that there was no significant difference of TWEAK expression when co-cultured with macrophages, indicating TRAF6 is on the upstream of TWEAK (Figure S5G). TRAF6 acts as an E3 ubiquitin ligase to form K63-type polyubiquitin chains (K63-Ub chains) and subsequently triggers NF-κB signaling activation.[36] E2 ubiquitin-conjugating (UBC) enzyme, UBE2O, inhibits TRAF6 polyubiquitination and the downstream components of NF-κB signaling.[37] We demonstrated that CCL5 promoted

(B) MuRF1, Atrogin-1, and RELB expression levels were investigated in C2C12 differentiated myotubes treated with recombinant TWEAK protein for 8 h.
(C) TWEAK expression in normal pancreas from the Sham group compared with that in tumor tissue from orthotopic KPC tumors. n = 2, 6/group; mean ± SD; **, $p < 0.01$ by t test.
(D) Representative images of IHC staining of mTWEAK in pancreatic cancer tissue of KPC GEMM mice. Scale bar represents 50 μm.
(E) Secretion of TWEAK was determined using ELISA assay with medium from KPC cells with or without co-culture with macrophages. "N.D." indicates non-detectable. n = 2; mean ± SD; ***, $p < 0.001$ by t test.
(F) Representative images of immunofluorescence staining of TWEAK and the biomarker of macrophage (CD68) and cancer cells (pan-CK) in the tumor tissue of mice bearing allograft tumor from KPC cells. Scale bar represents 10 μm.
(G) Protein expression levels of TWEAK were detected in KPC and AsPC-1 cells with or without co-cultured with macrophages. Mφ represents macrophages.
(H) The expression of TWEAK in PDX46 and PDX87 primary pancreatic cancer cells with or without co-culture with macrophages.
(I) Protein expression levels of TWEAK in KPC and AsPC-1 cells treated with the conditioned medium from macrophages or CCL2-treated macrophages.
(J) MuRF1 and Atrogin-1 expression levels were investigated in C2C12 differentiated myotubes treated with conditioned medium of KPC-siNC/siTWEAK with or without co-cultured with macrophages. siTW indicates siTWEAK.
(K) The expression of muscle wasting markers in C2C12 differentiated myotubes treated with conditioned medium from PDX46 and PDX87 cells co-cultured with macrophages.
(L) TWEAK protein levels in the tumor tissue of WT and *Ccr2*$^{-/-}$ transgenic mice bearing allograft tumors from KPC cells was evaluated by WB. n = 5/group; mean ± SD; **, $p < 0.01$ by t test. See also Figure S3.

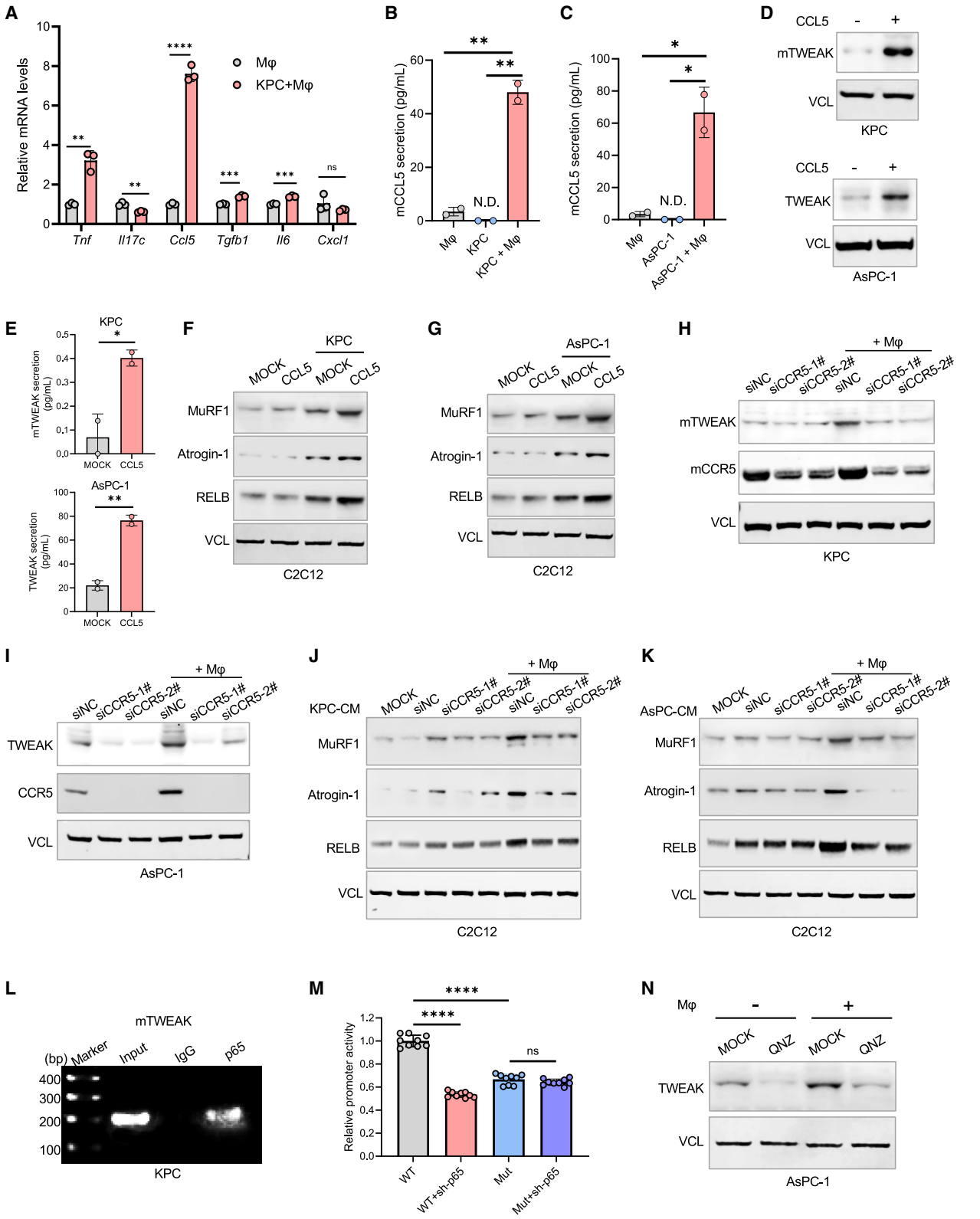

Figure 4. Macrophages derived CCL5 upregulates TWEAK via p65 signaling in pancreatic cancer

(A) The mRNA levels of cytokines in macrophages alone or co-cultured with KPC cells. n = 3/group; mean ± SD; **, $p < 0.01$, ***, $p < 0.001$; ****, $p < 0.0001$; ns, not significant by t test.

(legend continued on next page)

K63-linked ubiquitination of TRAF6 by inhibiting the interaction between TRAF6 and UBE2O, leading to TRAF6 polyubiquitination and NF-κB activation (Figure 5M). Therefore, these results indicated that macrophages facilitate cancer cachexia through activating TRAF6 K63-linked ubiquitination, resulting in the activation of NF-κB-TWEAK signaling pathway.

CCL2-activated macrophages induce muscle wasting in pancreatic cancer

We performed flow cytometry and found that the percentage of TAMs (M2) significantly decreased in the tumor tissue of non-CAC group compared to the CAC group (Figures 6A and S6A–S6C). Notably, we found no significant difference for T cell infiltration (Figure S6D). The percentage of CD206 positive cells was significantly increased in macrophages treated with the conditioned medium derived from KPC-CAC cells, whereas minimal effect was found in the non-CAC group. Similar results were obtained from AsPC-1 cells (Figure 6B). The conditioned medium from CAC cells that were co-cultured with macrophages increased muscle wasting biomarkers MuRF1 and Atrogin-1 expression in C2C12 differentiated myotubes, whereas minimal effect was found in non-CAC cells (Figure 6C). To determine key cytokines that contribute to cancer-induced macrophage recruitment and polarization, we evaluated the mRNA levels of several cytokines associated with macrophage recruitment in CAC and non-CAC cells. We found that CCL2 was the most significantly decreased cytokine in non-CAC cells compared to CAC cells (Figures 6D–6F and S6E). To further examine whether CCL2 is a major regulator of cancer-mediated macrophage recruitment and polarization, we used recombinant protein CCL2 to treat non-CAC cells and found that CCL2 restored the chemotactic migration ability of macrophages (Figure 6G). Additionally, treatment with CCL2 recombinant protein significantly restored the levels of CD206 and increased *Mrc1* and *Ccl5* expression in macrophages (Figure 6H, S6F–S6H). The expression of TWEAK was upregulated in pancreatic cancer cells when treated with conditioned medium derived from CCL2-activated macrophages (Figure 6I). Furthermore, MuRF1 and Atrogin-1 were upregulated in C2C12 differentiated myotubes treated with conditioned medium from cancer cells that were preconditioned by CCL2-activated macrophages (Figure 6J). CCL2-activated macrophages also promoted p65 activation in pancreatic cancer cells (Figure S6I). CCL2 alone did not increase the expression of muscle wasting markers MuRF1 and Atrogin-1 (Figure S6J). Taken together, these findings demonstrated that CCL2 activated macrophages induced muscle wasting in pancreatic cancer.

We then sought to examine the underlying mechanism of how pancreatic cancer upregulates CCL2. Previous studies suggest that several transcription factors including c-JUN, EGR1, ZXDC, and STAT3 activate CCL2.[38–41] To determine the putative transcription factors that mediate CCL2 expression in pancreatic cancer, we analyzed the mRNA levels of these genes in CAC and non-CAC cells (Figure S6K) and then focused on ZXDC, a zinc-dependent transcription factor. We found that ZXDC was significantly downregulated both at the mRNA and protein level in non-CAC cells compared to CAC cells. (Figure S6L). Knockdown of ZXDC reduced the CCL2 expression and secretion in KPC cells (Figures S6M–S6O). ChIP assay demonstrated that ZXDC binds to the promoter region of CCL2 and the binding was reduced in non-CAC cells (Figure S6P). These findings indicated that pancreatic cancer promoted macrophage recruitment and polarization through CCL2 which might be transcriptionally activated by ZXDC.

Cancer induced muscle wasting is partially dependent on the non-autonomous activation of TWEAK

To validate the critical role of non-autonomous activation of TWEAK in promoting cancer cachexia, we analyzed the secretion levels of multiple cytokines that are associated with cancer cachexia in the tumor tissue of KPC-CAC/non-CAC group using the cytokine antibody array. Several cytokines were downregulated in non-CAC group. Among these candidates, TWEAK was one of the top downregulated cytokines in non-CAC group compared to that in CAC group (Figures 7A and S7A). We further validated that protein level of TWEAK was higher in CAC group compared to that in the non-CAC group (Figures 7B, 7C and S7B). Macrophages co-culture further increased the level of TWEAK in tumor cells (Figures S7C–S7E). To further determine the role of TWEAK in cancer-induced muscle wasting, we established CAC-V, non-CAC-V, and non-CAC-TWEAK stable cell lines in both KPC and AsPC-1 cells (Figures S7F and S7G). TWEAK overexpression in both KPC and AsPC-1 non-CAC cells increased levels of muscle wasting markers Atrogin-1 and MuRF1 (Figures 7D and 7E). Besides the 2D pancreatic cancer cell culture model, we also established the 3D cancer spheroid model and validated that TWEAK increased the expression of MuRF1 in C2C12 differentiated myotubes (Figure S7H). Next, we evaluated the role of TWEAK in tumor growth and muscle atrophy *in vivo*. Overexpression of TWEAK did not affect tumor

(B and C) CCL5 secretion levels were measured in macrophages, KPC and AsPC-1 cells with or without co-culture with macrophages. "N.D." indicates non-detectable. n = 2/group; mean ± SD; *, $p < 0.05$, **, $p < 0.01$ by t test.
(D) Protein levels of TWEAK in KPC and AsPC-1 cells treated with recombinant protein CCL5 at 10 ng/mL for 72 h.
(E) TWEAK secretion levels in KPC and AsPC-1 cells treated with recombinant protein CCL5 at 10 ng/mL for 72 h. n = 2/group; mean ± SD; *, $p < 0.05$, **, $p < 0.01$ by t test.
(F and G) The expression levels of muscle atrophy markers MuRF1 and Atrogin-1 were examined in C2C12 myotubes treated with recombinant protein CCL5 or conditioned medium of KPC or AsPC-1 cells treated with CCL5.
(H and I) Knockdown of CCR5 by siRNAs in pancreatic cancer cells and evaluate the expression of TWEAK.
(J and K) Knockdown of CCR5 by siRNAs in pancreatic cancer cells and the condition medium was collected from the above cells to treat and evaluate the expression of muscle wasting markers in C2C12 differentiated myotubes.
(L) ChIP binding assay with anti-p65 to examine the binding of p65 to TWEAK promoter region in KPC cells.
(M) Luciferase reporter assay to examine whether p65 transcriptionally activates TWEAK. n = 9/group; mean ± SD; ****, $p < 0.0001$; ns, not significant by t test.
(N) TWEAK protein levels in AsPC-1 cells with or without the co-culture with macrophages and treatment with small molecule inhibitor of NF-κB (QNZ, 10 μM) for 48 h. See also Figure S4.

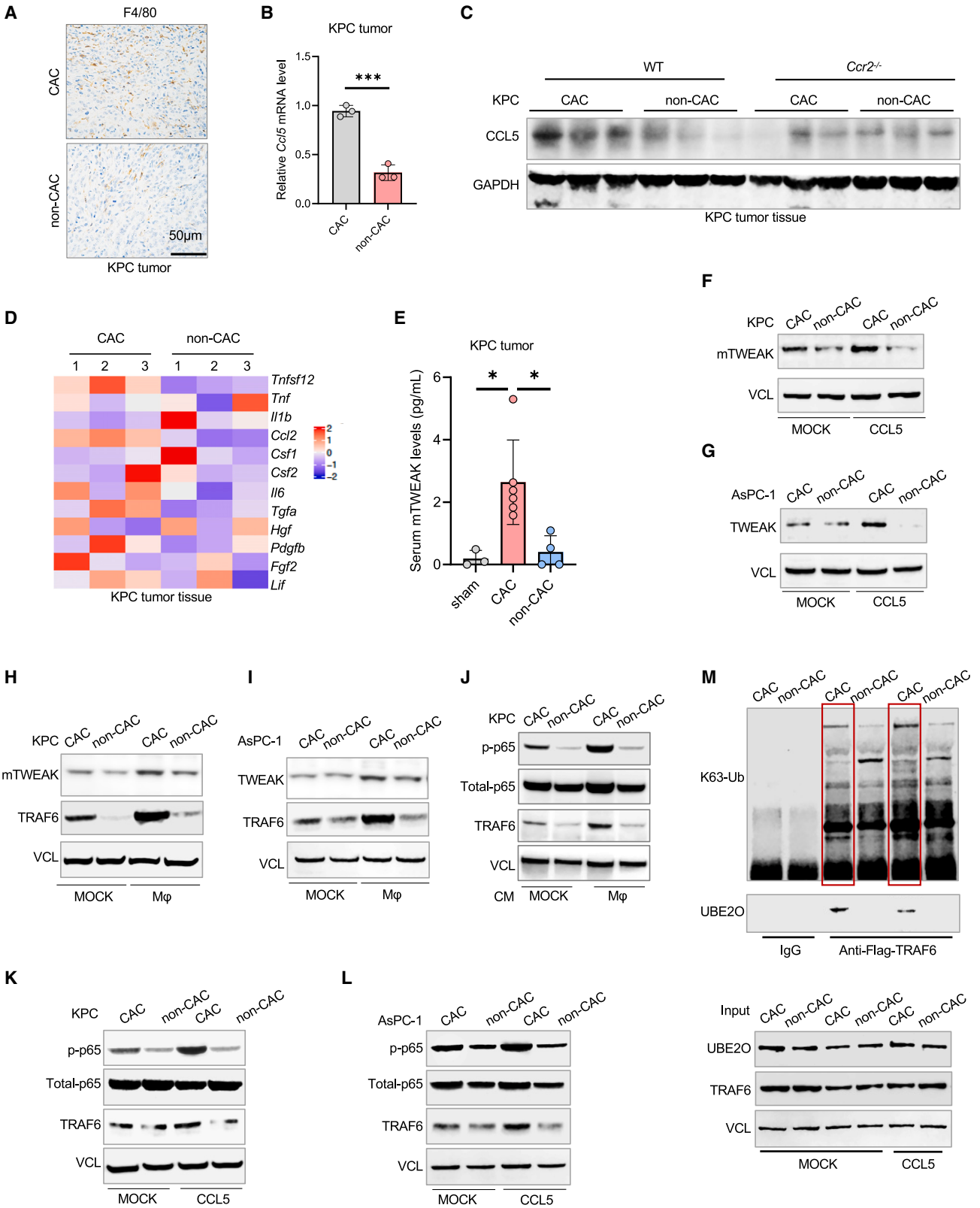

Figure 5. The non-autonomous activation of TWEAK is regulated via TRAF6/p65 pathway

(A) Representative images of IHC staining of F4/80 in orthotopic pancreatic cancer mouse model implanted with KPC-CAC and KPC-non-CAC cells. The scale bar is 50 μm.

(legend continued on next page)

growth (Figure S7I). *Ccr2* knockout in mice resulted in the attenuation of muscle wasting induced by CAC cells. Overexpression of TWEAK in non-CAC cells restored the muscle wasting phenotype in WT and *Ccr2*$^{-/-}$ mice (Figures 7F–7H). In addition, we found that TWEAK overexpression increased the expression of muscle wasting-associated markers, Atrogin-1 and MuRF1 in the TA muscle tissue from both C57BL/6 WT and *Ccr2*$^{-/-}$ mice (Figure 7I). Collectively, both *in vitro* and *in vivo* data suggest that non-autonomous activation of TWEAK is required for cancer-induced muscle wasting in pancreatic cancer.

TWEAK expression is associated with cancer cachexia in patients with pancreatic cancer

To validate the clinical significance of the macrophage-activated TWEAK signaling pathway in pancreatic cancer, we performed IHC staining and analyzed the expression of TWEAK, CD68 in human pancreatic tumor tissue, and MuRF1 in the paired muscle tissues. Patients with severe cachexia (defined as body weight loss greater than 10%) showed higher expression of TWEAK and CD68 in tumor tissue and higher expression of MuRF1 in muscle tissue compared to that in patients with less severe cachexia (Figures 8A and S8A). These findings indicated that the combination of TWEAK expression and macrophages infiltration could identify patients with increased risk of developing muscle wasting in pancreatic cancer. In summary, this study identified an essential role of macrophages in promoting cancer cachexia. Specifically, the non-autonomous activation of TWEAK induced by the crosstalk between tumor cells and macrophages drives pancreatic cancer cachexia through MuRF1-mediated muscle remodeling (Figure 8B).

DISCUSSION

Pancreatic cancer represents a poor-prognosis malignancy, with the highest prevalence of cancer cachexia.[4,42] Cachexia influences quality of life and overall survival among individuals with pancreatic cancer.[43] Unfortunately, treatment options are limited for the management of cancer cachexia.[7] Therefore, identifying potential therapeutic targets remains a challenge to effectively address cancer cachexia. In prior work, we identified that the dysregulation of the zinc signaling axis represents a critical regulator for tumor growth, metastasis, and chemoresistance in pancreatic cancer.[44,45] Further, we have found that a zinc-dependent transcription factor (i.e., CREB) promotes muscle wasting and cancer cachexia via TGF-β and TNF pathways.[22,24] However, the role of tumor microenvironment in promoting cancer cachexia remains poorly understood. In this study, we bridge this gap by identifying the crosstalk between tumor cells and macrophages that drives muscle wasting in pancreatic cancer.

Macrophages are among the most abundant cell types in the stroma of pancreatic cancer tissue, playing a critical role in driving pancreatic cancer progression.[46,47] However, the underlying mechanism of cancer-mediated cachexia involving the crosstalk between cancer cells and macrophages was underexplored. Previous studies involving muscle biopsy samples from patients with pancreatic cancer showed an inverse correlation between the density of macrophages in muscle tissue and the size of muscle fiber.[48] Increased infiltration of macrophages has been shown to be prevalent in adipose tissue of hepatocellular carcinoma, pancreatic cancer, and lung cancer mouse models, leading to adipose loss and cancer cachexia.[49,50] In our current study, we found substantial increase in macrophages in pancreatic tumor tissue, which correlated with muscle wasting. Conditioned medium from pancreatic cancer cells co-cultured with macrophages significantly upregulated MuRF1 and Atrogin-1 expression in C2C12 differentiated myotubes. Mechanism study demonstrated that pancreatic cancer cells promote cancer cachexia by inducing macrophages infiltration through ZXDC/CCL2 pathway. Interestingly, Kupffer cells, macrophages that are localized in the liver, play critical roles in cancer progression.[51] Kupffer cells promote pancreatic cancer progression by secreting TGF-β.[52] Our recent study showed that TGF-β promotes pancreatic cancer cachexia,[22] suggesting a potential interaction between liver and muscle via TGF-β pathway. Recently, a study showed that tumor EVPs educated Kupffer cells to increase the secretion of TNF.[53] Our current study revealed an important role of TWEAK (TNFSF12), a member of TNF family in cachexia. This study indicated that TWEAK mediates the pro-cachexia effect of macrophages and suggested potential crosstalk between Kupffer cells and muscle cells. Taken together, these findings demonstrate that Kupffer cells may play a role in cancer cachexia-associated muscle wasting by secreting TNF and TGF-β.

CCL5, also known as RANTES (regulated on activation, normal T cell expressed and secreted), has been shown to contribute to tumor growth, metastasis, and the formation of an immunosuppressive microenvironment.[54–56] Emerging evidence suggests that tumor-associated macrophages are a major source of CCL5, which establishes a potent paracrine regulatory circuit for tumor progression.[57,58] CCL5 from macrophages promotes tumor progression via CC receptor 5 (CCR5) in gastric cancer and glioma.[59,60] However, the role of CCL5 in pancreatic cancer cachexia has remained poorly defined. In this study, we found that pancreatic cancer cells upregulated CCL5 expression in macrophages. Macrophage-derived CCL5 promoted pancreatic

(B) *Ccl5* mRNA levels in the tumor tissue of KPC-CAC and KPC-non-CAC group. n = 3/group; mean ± SD; ***, $p < 0.001$ by t test.
(C) CCL5 protein levels in the tumor tissue of WT and *Ccr2*$^{-/-}$ transgenic mice bearing allograft tumors from KPC-CAC and KPC-non-CAC cells.
(D) mRNA levels of cancer cachexia associated genes were detected in the tumor tissue of KPC-CAC and KPC-non-CAC group.
(E) The levels of TWEAK in mice serum were detected by ELISA. n = 3, 6, 4/group; mean ± SD; *, $p < 0.05$ by t test.
(F and G) TWEAK protein levels in CAC and non-CAC cells treated with recombinant CCL5 at 10 ng/mL for 72 h.
(H and I) The expression of TWEAK and TRAF6 in CAC and non-CAC cells with or without co-cultured with macrophage.
(J) Expression of p-p65, total p65 and TRAF6 in CAC and non-CAC cells treated with conditioned medium from M2 macrophages.
(K and L) Protein levels of p-p65, total p65, and TRAF6 in CAC and non-CAC cells treated with recombinant mouse protein CCL5 at 10 ng/mL for 72 h.
(M) TRAF6 K63-ubiquitination and the association of TRAF6 and UBE2O were measured in TRAF6 overexpressing KPC-CAC and KPC-non-CAC cells treated with recombinant mouse protein CCL5. See also Figure S5.

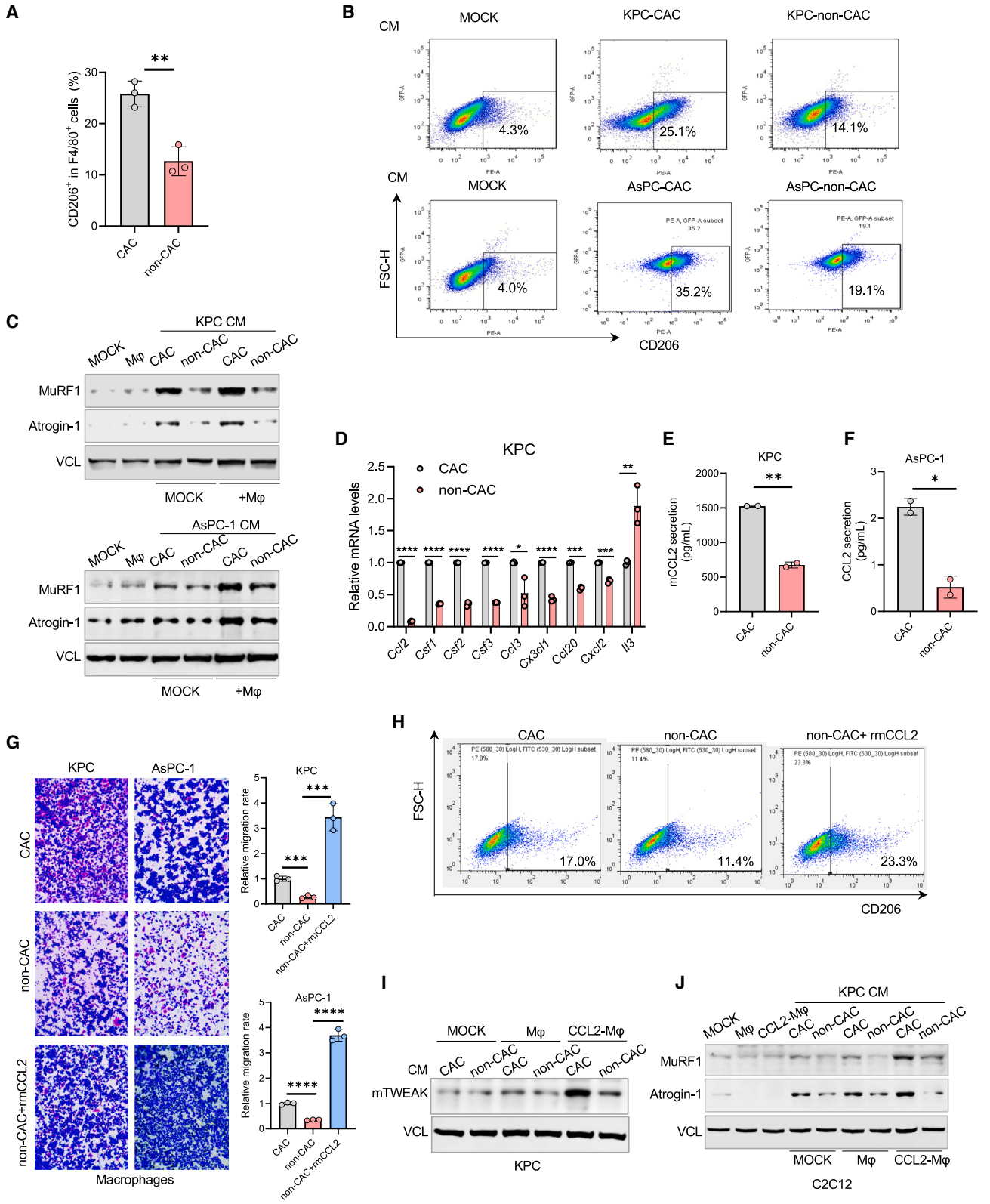

Figure 6. Pancreatic cancer activates macrophages induced muscle wasting through CCL2

(A) The percentage of M2 macrophages infiltration in the tumor tissue of CAC (n = 3) and non-CAC (n = 3) group was detected by flow cytometry analysis. n = 3/group; mean ± SD; **, $p < 0.01$ by t test.

(legend continued on next page)

cancer progression by activating TRAF6 and phosphorylating NF-κB subunit p65. Taken together, our findings support that pancreatic cancer cells activate tumor-associated macrophages via CCL2 and macrophages promote cancer progression via CCL5.

TWEAK is a pro-inflammation cytokine of the TNF family, which has been identified as a key regulator for muscle atrophy.[61,62] TWEAK promotes denervation-induced muscle atrophy in several neuromuscular disorders.[63–65] Dogra et al. elucidated that muscle specific TWEAK knocked-in mice exhibited severe loss of muscle mass at the neonatal stage.[66] Knockout of TWEAK inhibited muscle wasting induced by denervation.[66] TWEAK binds to its receptor fibroblast growth factor inducible 14 (Fn14) to activate non-canonical NF-κB pathway and induces muscle atrophy.[61,67] TWEAK/Fn14 axis is also essential for muscle regeneration. However, the mechanism of TWEAK upregulation in pancreatic cancer had previously remained unknown. Here, we found that pancreatic cancer upregulated TWEAK through the activation of NF-κB signaling pathway. We further characterized the role of macrophages in mediating pancreatic cancer cell-induced muscle wasting through TWEAK. Specifically, the crosstalk between tumor cells and macrophages increased the secretion of TWEAK, the latter of which induced muscle wasting. This was evident by the increase of muscle atrophy-associated markers Atrogin-1 and MuRF1 in C2C12 differentiated myotubes treated with recombinant TWEAK protein or conditioned medium from TWEAK-overexpressing pancreatic cancer cells. Our findings demonstrate that the crosstalk between tumor cells and macrophages results in the upregulation of TWEAK from tumor cells, leading to muscle wasting and cancer cachexia in pancreatic cancer. Antibody-drug conjugate targeting TWEAK signaling axis showed promising results in the preclinical settings of lung cancer.[68] Several monoclonal antibodies and small molecule antagonists that block TWEAK and CCL2 signaling axis have been developed for the treatment of pancreatic cancer and other cancers in the clinical settings.[69,70] These studies echo the translational potential of targeting CCL2-TWEAK signaling axis for the treatment of pancreatic cancer cachexia.

This study also has several limitations. The correlation between cachexia and immune cells in tumor tissue was initially analyzed using different datasets and was then validated in an independent cohort of pancreatic cancer patients. Future study is warranted to validate this finding in a larger cohort. Previous studies showed that *Ccr2*$^{-/-}$ mice had significantly lower levels of macrophages in the lung and liver tissue, while the level of neutrophils increased.[71–78] More studies are needed to examine how the balance of different immune cells will regulate cancer cachexia. Besides, the mechanism of CCL2 upregulation in tumor cells warrants further study.

In summary, this study identified a previously uncharacterized mechanism of pancreatic cancer cell-mediated muscle wasting through reprogramming of tumor-associated macrophages. Specifically, macrophages promoted non-autonomous activation of TWEAK from tumor cells via the CCL5/TRAF6/NF-κB signaling axis. Meanwhile, tumor cells recruited and activated macrophages via CCL2, establishing a positive crosstalk between pancreatic cancer cells and macrophages. The upregulated TWEAK promoted muscle wasting through the MuRF1 signaling pathway. Ultimately, these findings provide promising therapeutic targets to inform future work seeking to address cancer cachexia in pancreatic cancer.

STAR★METHODS

Detailed methods are provided in the online version of this paper and include the following:

- KEY RESOURCES TABLE
- RESOURCE AVAILABILITY
  - Lead contact
  - Materials availability
  - Data and code availability
- EXPERIMENTAL MODEL AND SUBJECT DETAILS
  - Cell lines
  - Transgenic mouse models
  - Clinical samples
- METHOD DETAILS
  - Stable cell line construction
  - Chromatin immunoprecipitation assay
  - Dual luciferase assay for promoter activity
  - Western blot analysis
  - Immunohistochemical staining
  - ELISA assay
  - In silico analysis
  - Pancreatic cancer allograft mouse models
- QUANTIFICATION AND STATISTICAL ANALYSIS

SUPPLEMENTAL INFORMATION

Supplemental information can be found online at https://doi.org/10.1016/j.ccell.2024.03.009.

(B) The percentage of CD206 positive cells in macrophages treated with the conditioned medium from CAC or non-CAC cells.
(C) Expression of muscle wasting protein MuRF1 and Atrogin-1 were detected in C2C12 differentiated myotubes treated with the conditioned medium from CAC and non-CAC cells with or without co-culture with macrophages.
(D) The mRNA levels of genes associated with macrophages recruitment were detected in CAC and non-CAC cells. n = 3/group; mean ± SD; *, $p < 0.05$; **, $p < 0.01$; ***; $p < 0.001$; ****; $p < 0.0001$ by t test.
(E and F) Secretion of CCL2 was measured using ELISA assay with supernatant of CAC or non-CAC cells. n = 2/group; mean ± SD; *, $p < 0.05$; **, $p < 0.01$ by t test.
(G) Chemotactic migration assays of macrophages using the supernatant of CAC or non-CAC cells in the presence CCL2 recombinant protein. n = 3/group; mean ± SD; ***, $p < 0.001$; ****, $p < 0.0001$ by t test.
(H) The percentage of CD206 positive cells in macrophages treated with the CCL2 or the conditioned medium from AsPC-CAC/non-CAC cells.
(I and J) CAC/non-CAC cells were treated with the conditioned medium from M0 or CCL2 activated M0 macrophages for 72 h, respectively and then detected the expression of TWEAK. The medium was collected and treated C2C12 differentiated myotube for 8 h and analyzed the expression of MuRF1 and Atrogin-1. See also Figure S6.

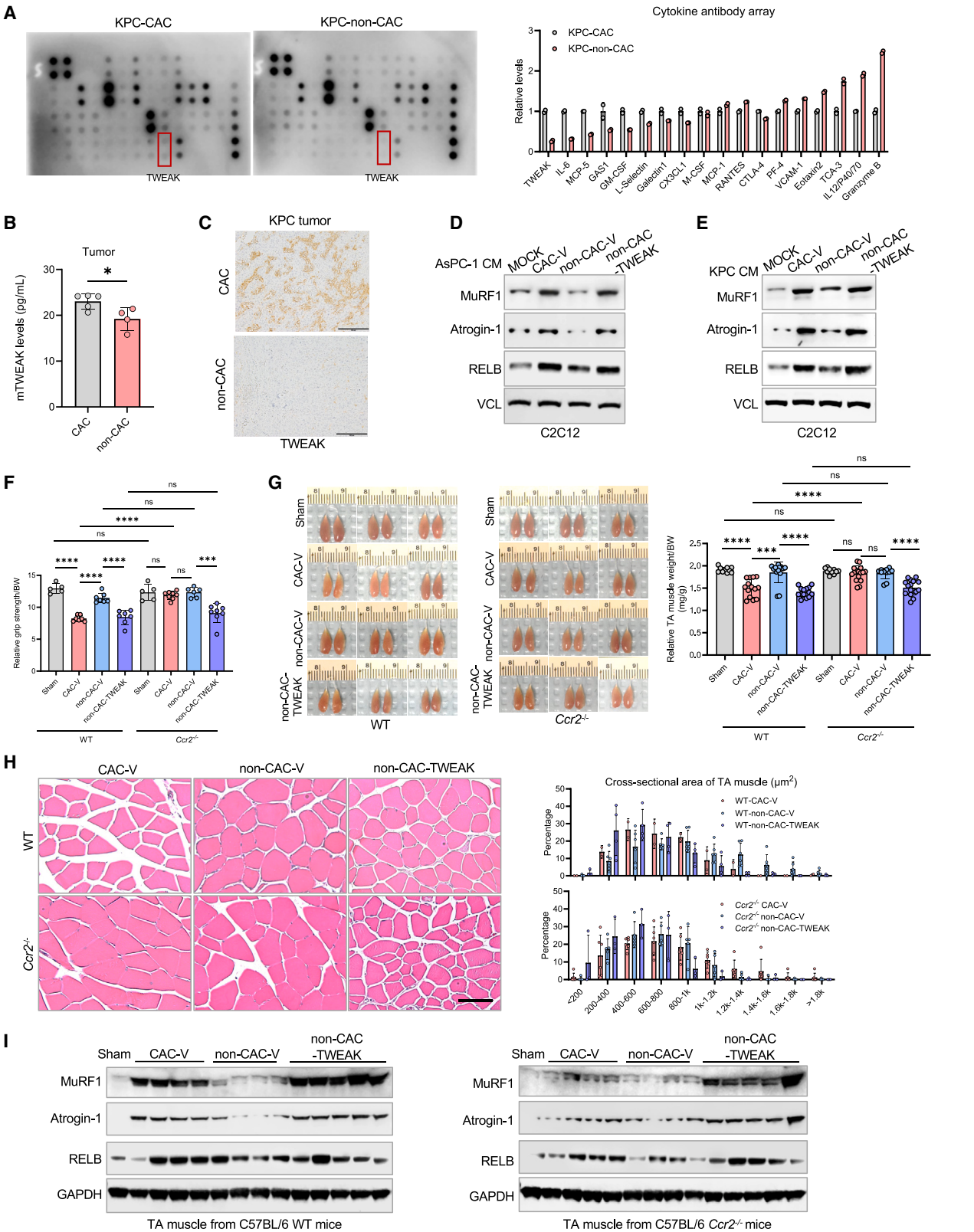

Figure 7. Cancer induced muscle wasting is partially dependent on the non-autonomous activation of TWEAK

(A) Protein levels of cancer cachexia associated genes were detected in the tumor tissue from KPC-CAC/non-CAC groups using cytokine antibody array.

(B) Secretion level of TWEAK in the tumor tissue of KPC-CAC/non-CAC groups. n = 5, 4/group; mean ± SD; *, $p < 0.05$ by t test.

(legend continued on next page)

ACKNOWLEDGMENTS

This work was supported in part by the National Institutes of Health National Cancer Institute grants R01 CA186338, R01 CA203108, R01 CA247234, and award P30 CA225520, and by the William and Ella Owens Medical Research Foundation (M. Li). The PDX cell lines derived from pancreatic cancer patients with cachexia were established by Dr. Jose Trevino from Virginia Commonwealth University.

AUTHOR CONTRIBUTIONS

Study conception and design: M.Liu, Y.R., Z.Z., J.Y., X.S., Y.Z., and M.Li. Data curation: M.Liu, Y.R., Z.Z., J.Y., Y.C., and X.S. Formal analysis: M.Liu, Y.R., Z.Z., J.Y., X.S., Y.C., C.X., K.F., A.A., and W.L. Visualization: M.Liu, Y.R., Z.Z., and J.Y. Resources: M.B., Y.Z., L.Z., C.H., Y.L., and M.Li. Funding acquisition: M.Li. Writing – original drafts: M.Liu, Y.R., and Z.Z. Writing – review and editing: M.Liu, Y.R., Z.Z., J.Y., X.S., R.N., A.A., M.B., Y.L., L.Z., C.H., Y.Z., and M.Li. Supervision: Y.Z. and M.Li.

DECLARATION OF INTERESTS

C.W. Houchen has ownership interest in COARE Holdings Inc.

Received: August 26, 2023
Revised: December 18, 2023
Accepted: March 15, 2024
Published: April 11, 2024

REFERENCES

1. Siegel, R.L., Miller, K.D., Wagle, N.S., and Jemal, A. (2023). Cancer statistics, 2023. CA. Cancer J. Clin. *73*, 17–48. https://doi.org/10.3322/caac.21763.
2. Rahib, L., Wehner, M.R., Matrisian, L.M., and Nead, K.T. (2021). Estimated Projection of US Cancer Incidence and Death to 2040. JAMA Netw. Open *4*, e214708. https://doi.org/10.1001/jamanetworkopen.2021.4708.
3. Mizrahi, J.D., Surana, R., Valle, J.W., and Shroff, R.T. (2020). Pancreatic cancer. Lancet *395*, 2008–2020. https://doi.org/10.1016/S0140-6736(20)30974-0.
4. Baracos, V.E., Martin, L., Korc, M., Guttridge, D.C., and Fearon, K.C.H. (2018). Cancer-associated cachexia. Nat. Rev. Dis. Primers *4*, 17105. https://doi.org/10.1038/nrdp.2017.105.
5. Pryce, B.R., Wang, D.J., Zimmers, T.A., Ostrowski, M.C., and Guttridge, D.C. (2023). Cancer cachexia: involvement of an expanding macroenvironment. Cancer Cell *41*, 581–584. https://doi.org/10.1016/j.ccell.2023.02.007.
6. Fearon, K., Strasser, F., Anker, S.D., Bosaeus, I., Bruera, E., Fainsinger, R.L., Jatoi, A., Loprinzi, C., MacDonald, N., Mantovani, G., et al. (2011). Definition and classification of cancer cachexia: an international consensus. Lancet Oncol. *12*, 489–495. https://doi.org/10.1016/S1470-2045(10)70218-7.
7. Roeland, E.J., Bohlke, K., Baracos, V.E., Bruera, E., Del Fabbro, E., Dixon, S., Fallon, M., Herrstedt, J., Lau, H., Platek, M., et al. (2020). Management of Cancer Cachexia: ASCO Guideline. J. Clin. Oncol. *38*, 2438–2453. https://doi.org/10.1200/JCO.20.00611.
8. Hosein, A.N., Brekken, R.A., and Maitra, A. (2020). Pancreatic cancer stroma: an update on therapeutic targeting strategies. Nat. Rev. Gastroenterol. Hepatol. *17*, 487–505. https://doi.org/10.1038/s41575-020-0300-1.
9. Huang, H., Wang, Z., Zhang, Y., Pradhan, R.N., Ganguly, D., Chandra, R., Murimwa, G., Wright, S., Gu, X., Maddipati, R., et al. (2022). Mesothelial cell-derived antigen-presenting cancer-associated fibroblasts induce expansion of regulatory T cells in pancreatic cancer. Cancer Cell *40*, 656–673.e7. https://doi.org/10.1016/j.ccell.2022.04.011.
10. Zhou, Z., Xia, G., Xiang, Z., Liu, M., Wei, Z., Yan, J., Chen, W., Zhu, J., Awasthi, N., Sun, X., et al. (2019). A C-X-C Chemokine Receptor Type 2-Dominated Cross-talk between Tumor Cells and Macrophages Drives Gastric Cancer Metastasis. Clin. Cancer Res. *25*, 3317–3328. https://doi.org/10.1158/1078-0432.CCR-18-3567.
11. Lee, B.Y., Hogg, E.K.J., Below, C.R., Kononov, A., Blanco-Gomez, A., Heider, F., Xu, J., Hutton, C., Zhang, X., Scheidt, T., et al. (2021). Heterocellular OSM-OSMR signalling reprograms fibroblasts to promote pancreatic cancer growth and metastasis. Nat. Commun. *12*, 7336. https://doi.org/10.1038/s41467-021-27607-8.
12. Pucci, F., and Coussens, L.M. (2021). Redirecting tumor macrophage activity to fight cancer: Make room for the next era of anti-cancer drugs. Cancer Cell *39*, 1300–1302. https://doi.org/10.1016/j.ccell.2021.09.009.
13. Madaro, L., Passafaro, M., Sala, D., Etxaniz, U., Lugarini, F., Proietti, D., Alfonsi, M.V., Nicoletti, C., Gatto, S., De Bardi, M., et al. (2018). Denervation-activated STAT3-IL-6 signalling in fibro-adipogenic progenitors promotes myofibres atrophy and fibrosis. Nat. Cell Biol. *20*, 917–927. https://doi.org/10.1038/s41556-018-0151-y.
14. Carr, R.M., and Fernandez-Zapico, M.E. (2020). It Takes a Village to Overcome KRAS Dependence in Pancreatic Cancer. Cancer Discov. *10*, 910–912. https://doi.org/10.1158/2159-8290.CD-20-0490.
15. Hou, P., Kapoor, A., Zhang, Q., Li, J., Wu, C.J., Li, J., Lan, Z., Tang, M., Ma, X., Ackroyd, J.J., et al. (2020). Tumor Microenvironment Remodeling Enables Bypass of Oncogenic KRAS Dependency in Pancreatic Cancer. Cancer Discov. *10*, 1058–1077. https://doi.org/10.1158/2159-8290.CD-19-0597.
16. Talbert, E.E., Lewis, H.L., Farren, M.R., Ramsey, M.L., Chakedis, J.M., Rajasekera, P., Haverick, E., Sarna, A., Bloomston, M., Pawlik, T.M., et al. (2018). Circulating monocyte chemoattractant protein-1 (MCP-1) is associated with cachexia in treatment-naive pancreatic cancer patients. J. Cachexia Sarcopenia Muscle *9*, 358–368. https://doi.org/10.1002/jcsm.12251.
17. Petruzzelli, M., and Wagner, E.F. (2016). Mechanisms of metabolic dysfunction in cancer-associated cachexia. Genes Dev. *30*, 489–501. https://doi.org/10.1101/gad.276733.115.
18. Argilés, J.M., Stemmler, B., López-Soriano, F.J., and Busquets, S. (2018). Inter-tissue communication in cancer cachexia. Nat. Rev. Endocrinol. *15*, 9–20. https://doi.org/10.1038/s41574-018-0123-0.
19. Poulia, K.A., Sarantis, P., Antoniadou, D., Koustas, E., Papadimitropoulou, A., Papavassiliou, A.G., and Karamouzis, M.V. (2020). Pancreatic Cancer

(C) IHC staining of mTWEAK expression in the tumor tissue of KPC-CAC/non-CAC groups. The scale bar is 100 μm.
(D and E) MuRF1, Atrogin-1, and RELB expression levels were investigated in C2C12 differentiated myotubes treated with conditioned medium of CAC-V, non-CAC-V and non-CAC-TWEAK cells from AsPC-1 and KPC cells, respectively.
(F) Relative grip strength of the WT (n = 5, 7, 7, 7/group) and *Ccr2*$^{-/-}$ mice (n = 5, 8, 6, 8/group) bearing allograft tumors from KPC-CAC-V, KPC-non-CAC-V, or KPC-non-CAC-TWEAK cells, respectively. Mean ± SD; ***; $p < 0.001$; ****; $p < 0.0001$; ns, not significant, by t test.
(G) Representative TA muscle images and relative muscle weight to body weight of WT (n = 10, 14, 14, 14/group) and *Ccr2*$^{-/-}$ mice (n = 10, 16, 12, 16/group) bearing allograft tumors from KPC-CAC-V, KPC-non-CAC-V, or KPC-non-CAC-TWEAK cells. Right, relative muscle weight to body weight. Mean ± SD; ***; $p < 0.001$; ****; $p < 0.0001$; ns, not significant, by t test.
(H) H&E staining of TA muscle sections of mice from experiment (G). The scale bar is 50 μm. Right, quantitative analysis of TA muscle cross-sectional area.
(I) Expression of muscle wasting protein MuRF1 and Atrogin-1 were detected in the TA muscle tissue of Sham, CAC-V, non-CAC-V, and non-CAC-TWEAK group in (G). See also Figure S7.

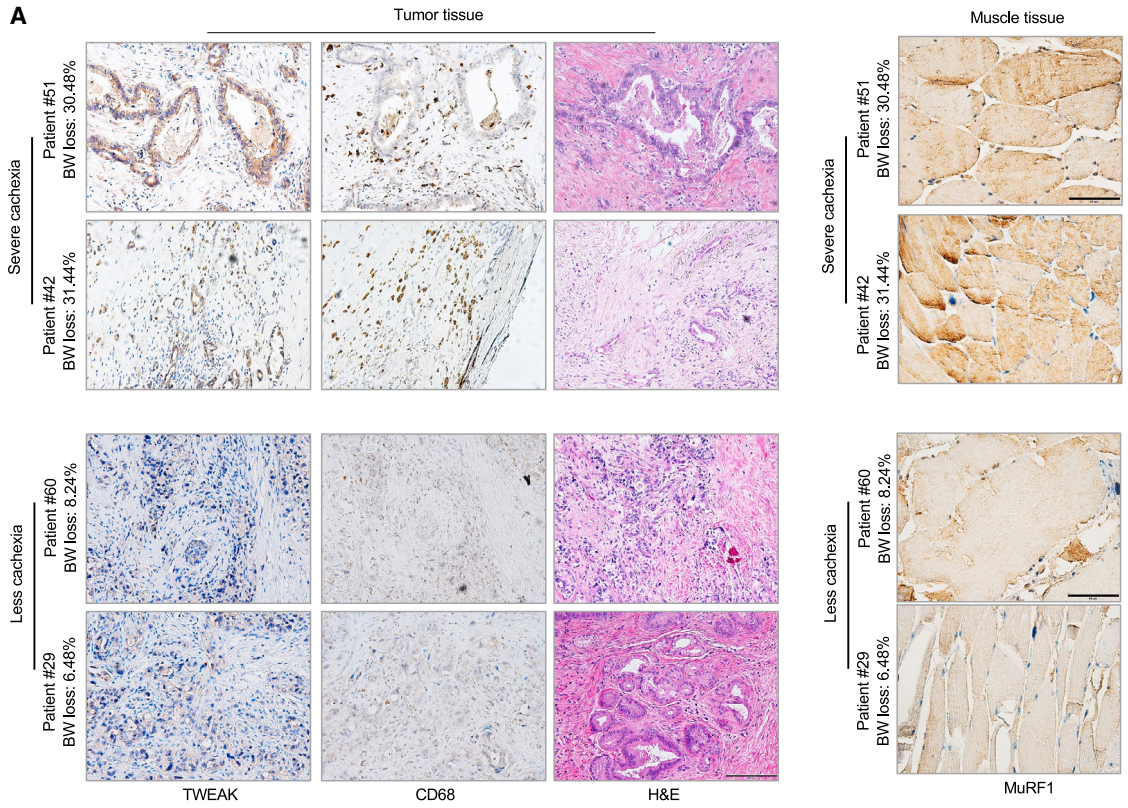

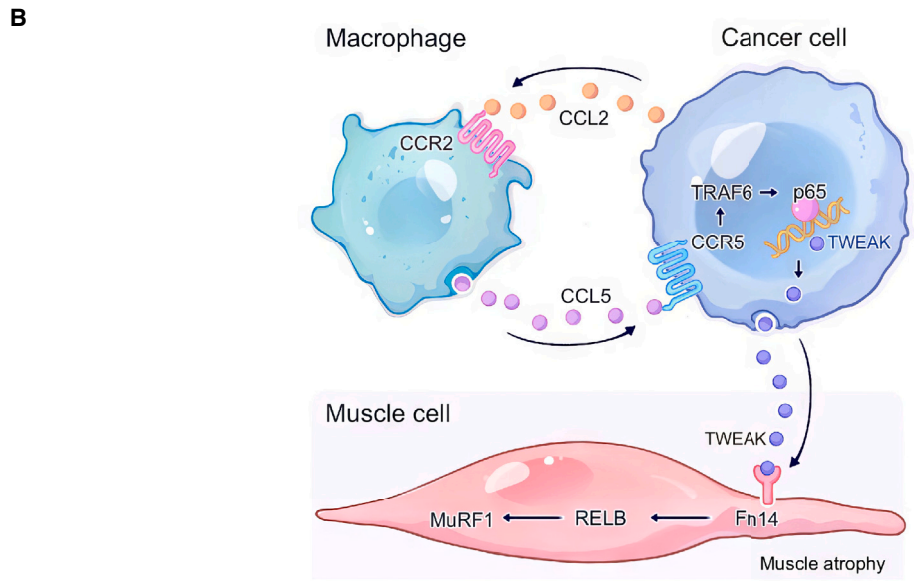

Figure 8. TWEAK expression is associated with cancer cachexia in patients with pancreatic cancer

(A) Representative IHC staining of CD68 and TWEAK in tumor tissues (scale bar represents 100 μm) and MuRF1 in muscle tissues (scale bar represents 50 μm) of patients with pancreatic cancer.

(B) Schematic diagram. Pancreatic cancer cells recruit macrophages through CCL2 signaling axis. Activated macrophages facilitate the secretion of TWEAK from tumor cells in a CCL5-TRAF6-p65 dependent manner. TWEAK activates RELB-MuRF1 signaling pathway in muscle myotubes, leading to cancer cachexia. See also Figure S8.

and Cachexia-Metabolic Mechanisms and Novel Insights. Nutrients *12*, 1543. https://doi.org/10.3390/nu12061543.

20. Hou, Y.C., Wang, C.J., Chao, Y.J., Chen, H.Y., Wang, H.C., Tung, H.L., Lin, J.T., and Shan, Y.S. (2018). Elevated Serum Interleukin-8 Level Correlates with Cancer-Related Cachexia and Sarcopenia: An Indicator for Pancreatic Cancer Outcomes. J. Clin. Med. *7*, 502. https://doi.org/10.3390/jcm7120502.
21. Tan, C.R., Yaffee, P.M., Jamil, L.H., Lo, S.K., Nissen, N., Pandol, S.J., Tuli, R., and Hendifar, A.E. (2014). Pancreatic cancer cachexia: a review of mechanisms and therapeutics. Front. Physiol. *5*, 88. https://doi.org/10.3389/fphys.2014.00088.
22. Shi, X., Yang, J., Liu, M., Zhang, Y., Zhou, Z., Luo, W., Fung, K.M., Xu, C., Bronze, M.S., Houchen, C.W., and Li, M. (2022). Circular RNA ANAPC7 Inhibits Tumor Growth and Muscle Wasting via PHLPP2-AKT-TGF-beta Signaling Axis in Pancreatic Cancer. Gastroenterology *162*, 2004–2017.e2. https://doi.org/10.1053/j.gastro.2022.02.017.
23. Yang, J., Zhang, Z., Zhang, Y., Ni, X., Zhang, G., Cui, X., Liu, M., Xu, C., Zhang, Q., Zhu, H., et al. (2019). ZIP4 Promotes Muscle Wasting and Cachexia in Mice With Orthotopic Pancreatic Tumors by Stimulating RAB27B-Regulated Release of Extracellular Vesicles From Cancer Cells. Gastroenterology *156*, 722–734.e6. https://doi.org/10.1053/j.gastro.2018.10.026.
24. Zhou, Z., Ren, Y., Yang, J., Liu, M., Shi, X., Luo, W., Fung, K.M., Xu, C., Bronze, M.S., Zhang, Y., et al. (2022). Acetyl-Coenzyme A Synthetase 2 Potentiates Macropinocytosis and Muscle Wasting Through Metabolic Reprogramming in Pancreatic Cancer. Gastroenterology *163*, 1281–1293.e1. https://doi.org/10.1053/j.gastro.2022.06.058.
25. Penafuerte, C.A., Gagnon, B., Sirois, J., Murphy, J., MacDonald, N., and Tremblay, M.L. (2016). Identification of neutrophil-derived proteases and angiotensin II as biomarkers of cancer cachexia. Br. J. Cancer *114*, 680–687. https://doi.org/10.1038/bjc.2016.3.
26. de Visser, K.E., and Joyce, J.A. (2023). The evolving tumor microenvironment: From cancer initiation to metastatic outgrowth. Cancer Cell *41*, 374–403. https://doi.org/10.1016/j.ccell.2023.02.016.
27. Freire, P.P., Fernandez, G.J., de Moraes, D., Cury, S.S., Dal Pai-Silva, M., Dos Reis, P.P., Rogatto, S.R., and Carvalho, R.F. (2020). The expression landscape of cachexia-inducing factors in human cancers. J. Cachexia Sarcopenia Muscle *11*, 947–961. https://doi.org/10.1002/jcsm.12565.
28. Cassetta, L., Fragkogianni, S., Sims, A.H., Swierczak, A., Forrester, L.M., Zhang, H., Soong, D.Y.H., Cotechini, T., Anur, P., Lin, E.Y., et al. (2019). Human Tumor-Associated Macrophage and Monocyte Transcriptional Landscapes Reveal Cancer-Specific Reprogramming, Biomarkers, and Therapeutic Targets. Cancer Cell *35*, 588–602.e10. https://doi.org/10.1016/j.ccell.2019.02.009.
29. Queiroz, A.L., Dantas, E., Ramsamooj, S., Murthy, A., Ahmed, M., Zunica, E.R.M., Liang, R.J., Murphy, J., Holman, C.D., Bare, C.J., et al. (2022). Blocking ActRIIB and restoring appetite reverses cachexia and improves survival in mice with lung cancer. Nat. Commun. *13*, 4633. https://doi.org/10.1038/s41467-022-32135-0.
30. Hara, T., Chanoch-Myers, R., Mathewson, N.D., Myskiw, C., Atta, L., Bussema, L., Eichhorn, S.W., Greenwald, A.C., Kinker, G.S., Rodman, C., et al. (2021). Interactions between cancer cells and immune cells drive transitions to mesenchymal-like states in glioblastoma. Cancer Cell *39*, 779–792.e11. https://doi.org/10.1016/j.ccell.2021.05.002.
31. Boring, L., Gosling, J., Chensue, S.W., Kunkel, S.L., Farese, R.V., Jr., Broxmeyer, H.E., and Charo, I.F. (1997). Impaired monocyte migration and reduced type 1 (Th1) cytokine responses in C-C chemokine receptor 2 knockout mice. J. Clin. Invest. *100*, 2552–2561. https://doi.org/10.1172/JCI119798.
32. Johnston, A.J., Murphy, K.T., Jenkinson, L., Laine, D., Emmrich, K., Faou, P., Weston, R., Jayatilleke, K.M., Schloegel, J., Talbo, G., et al. (2015). Targeting of Fn14 Prevents Cancer-Induced Cachexia and Prolongs Survival. Cell *162*, 1365–1378. https://doi.org/10.1016/j.cell.2015.08.031.
33. Wu, H.Y., Trevino, J.G., Fang, B.L., Riner, A.N., Vudatha, V., Zhang, G.H., and Li, Y.P. (2022). Patient-Derived Pancreatic Cancer Cells Induce C2C12 Myotube Atrophy by Releasing Hsp70 and Hsp90. Cells *11*, 2756. https://doi.org/10.3390/cells11172756.
34. Walens, A., DiMarco, A.V., Lupo, R., Kroger, B.R., Damrauer, J.S., and Alvarez, J.V. (2019). CCL5 promotes breast cancer recurrence through macrophage recruitment in residual tumors. Elife *8*, e43653. https://doi.org/10.7554/eLife.43653.
35. He, W.A., Berardi, E., Cardillo, V.M., Acharyya, S., Aulino, P., Thomas-Ahner, J., Wang, J., Bloomston, M., Muscarella, P., Nau, P., et al. (2013). NF-kappaB-mediated Pax7 dysregulation in the muscle microenvironment promotes cancer cachexia. J. Clin. Invest. *123*, 4821–4835. https://doi.org/10.1172/JCI68523.
36. Xie, C., Zhang, L.Z., Chen, Z.L., Zhong, W.J., Fang, J.H., Zhu, Y., Xiao, M.H., Guo, Z.W., Zhao, N., He, X., and Zhuang, S.M. (2020). A hMTR4-PDIA3P1-miR-125/124-TRAF6 Regulatory Axis and Its Function in NF kappa B Signaling and Chemoresistance. Hepatology *71*, 1660–1677. https://doi.org/10.1002/hep.30931.
37. Zhang, X., Zhang, J., Zhang, L., van Dam, H., and ten Dijke, P. (2013). UBE2O negatively regulates TRAF6-mediated NF-kappaB activation by inhibiting TRAF6 polyubiquitination. Cell Res. *23*, 366–377. https://doi.org/10.1038/cr.2013.21.
38. Liu, C., Luan, S., OuYang, H., Huang, Z., Wu, S., Ma, C., Wei, J., and Xin, W. (2016). Upregulation of CCL2 via ATF3/c-Jun interaction mediated the Bortezomib-induced peripheral neuropathy. Brain Behav. Immun. *53*, 96–104. https://doi.org/10.1016/j.bbi.2015.11.004.
39. Maekawa, T., Takahashi, N., Honda, T., Yonezawa, D., Miyashita, H., Okui, T., Tabeta, K., and Yamazaki, K. (2010). Porphyromonas gingivalis antigens and interleukin-6 stimulate the production of monocyte chemoattractant protein-1 via the upregulation of early growth response-1 transcription in human coronary artery endothelial cells. J. Vasc. Res. *47*, 346–354. https://doi.org/10.1159/000265568.
40. Ramsey, J.E., and Fontes, J.D. (2013). The zinc finger transcription factor ZXDC activates CCL2 gene expression by opposing BCL6-mediated repression. Mol. Immunol. *56*, 768–780. https://doi.org/10.1016/j.molimm.2013.07.001.
41. Yang, X., Lin, Y., Shi, Y., Li, B., Liu, W., Yin, W., Dang, Y., Chu, Y., Fan, J., and He, R. (2016). FAP Promotes Immunosuppression by Cancer-Associated Fibroblasts in the Tumor Microenvironment via STAT3-CCL2 Signaling. Cancer Res. *76*, 4124–4135. https://doi.org/10.1158/0008-5472.CAN-15-2973.
42. Wood, L.D., Canto, M.I., Jaffee, E.M., and Simeone, D.M. (2022). Pancreatic Cancer: Pathogenesis, Screening, Diagnosis, and Treatment. Gastroenterology *163*, 386–402.e1. https://doi.org/10.1053/j.gastro.2022.03.056.
43. Tuca, A., Jimenez-Fonseca, P., and Gascón, P. (2013). Clinical evaluation and optimal management of cancer cachexia. Crit. Rev. Oncol. Hematol. *88*, 625–636. https://doi.org/10.1016/j.critrevonc.2013.07.015.
44. Li, M., Zhang, Y., Liu, Z., Bharadwaj, U., Wang, H., Wang, X., Zhang, S., Liuzzi, J.P., Chang, S.M., Cousins, R.J., et al. (2007). Aberrant expression of zinc transporter ZIP4 (SLC39A4) significantly contributes to human pancreatic cancer pathogenesis and progression. Proc. Natl. Acad. Sci. USA *104*, 18636–18641. https://doi.org/10.1073/pnas.0709307104.
45. Liu, M., Zhang, Y., Yang, J., Cui, X., Zhou, Z., Zhan, H., Ding, K., Tian, X., Yang, Z., Fung, K.A., et al. (2020). ZIP4 Increases Expression of Transcription Factor ZEB1 to Promote Integrin alpha3beta1 Signaling and Inhibit Expression of the Gemcitabine Transporter ENT1 in Pancreatic Cancer Cells. Gastroenterology *158*, 679–692.e671. https://doi.org/10.1053/j.gastro.2019.10.038.
46. Zhu, Y., Herndon, J.M., Sojka, D.K., Kim, K.W., Knolhoff, B.L., Zuo, C., Cullinan, D.R., Luo, J., Bearden, A.R., Lavine, K.J., et al. (2017). Tissue-Resident Macrophages in Pancreatic Ductal Adenocarcinoma Originate from Embryonic Hematopoiesis and Promote Tumor Progression. Immunity *47*, 323–338.e6. https://doi.org/10.1016/j.immuni.2017.07.014.
47. Liu, X., Hogg, G.D., Zuo, C., Borcherding, N.C., Baer, J.M., Lander, V.E., Kang, L.I., Knolhoff, B.L., Ahmad, F., Osterhout, R.E., et al. (2023). Context-dependent activation of STING-interferon signaling by CD11b

agonists enhances anti-tumor immunity. Cancer Cell *41*, 1073–1090.e12. https://doi.org/10.1016/j.ccell.2023.04.018.

48. Shukla, S.K., Markov, S.D., Attri, K.S., Vernucci, E., King, R.J., Dasgupta, A., Grandgenett, P.M., Hollingsworth, M.A., Singh, P.K., Yu, F., and Mehla, K. (2020). Macrophages potentiate STAT3 signaling in skeletal muscles and regulate pancreatic cancer cachexia. Cancer Lett. *484*, 29–39. https://doi.org/10.1016/j.canlet.2020.04.017.
49. Lu, S.W., Pan, H.C., Hsu, Y.H., Chang, K.C., Wu, L.W., Chen, W.Y., and Chang, M.S. (2020). IL-20 antagonist suppresses PD-L1 expression and prolongs survival in pancreatic cancer models. Nat. Commun. *11*, 4611. https://doi.org/10.1038/s41467-020-18244-8.
50. Markov, S.D., Gonzalez, D., and Mehla, K. (2020). Preclinical Models for Studying the Impact of Macrophages on Cancer Cachexia. Curr. Protoc. Pharmacol. *91*, e80. https://doi.org/10.1002/cpph.80.
51. Kerzel, T., Giacca, G., Beretta, S., Bresesti, C., Notaro, M., Scotti, G.M., Balestrieri, C., Canu, T., Redegalli, M., Pedica, F., et al. (2023). In vivo macrophage engineering reshapes the tumor microenvironment leading to eradication of liver metastases. Cancer Cell *41*, 1892–1910.e10. https://doi.org/10.1016/j.ccell.2023.09.014.
52. Costa-Silva, B., Aiello, N.M., Ocean, A.J., Singh, S., Zhang, H., Thakur, B.K., Becker, A., Hoshino, A., Mark, M.T., Molina, H., et al. (2015). Pancreatic cancer exosomes initiate pre-metastatic niche formation in the liver. Nat. Cell Biol. *17*, 816–826. https://doi.org/10.1038/ncb3169.
53. Wang, G., Li, J., Bojmar, L., Chen, H., Li, Z., Tobias, G.C., Hu, M., Homan, E.A., Lucotti, S., Zhao, F., et al. (2023). Tumour extracellular vesicles and particles induce liver metabolic dysfunction. Nature *618*, 374–382. https://doi.org/10.1038/s41586-023-06114-4.
54. Dangaj, D., Bruand, M., Grimm, A.J., Ronet, C., Barras, D., Duttagupta, P.A., Lanitis, E., Duraiswamy, J., Tanyi, J.L., Benencia, F., et al. (2019). Cooperation between Constitutive and Inducible Chemokines Enables T Cell Engraftment and Immune Attack in Solid Tumors. Cancer Cell *35*, 885–900.e10. https://doi.org/10.1016/j.ccell.2019.05.004.
55. Bauer, L., Hapfelmeier, A., Blank, S., Reiche, M., Slotta-Huspenina, J., Jesinghaus, M., Novotny, A., Schmidt, T., Grosser, B., Kohlruss, M., et al. (2018). A novel pretherapeutic gene expression-based risk score for treatment guidance in gastric cancer. Ann. Oncol. *29*, 127–132. https://doi.org/10.1093/annonc/mdx685.
56. Huang, C., Li, Z., Li, N., Li, Y., Chang, A., Zhao, T., Wang, X., Wang, H., Gao, S., Yang, S., et al. (2018). Interleukin 35 Expression Correlates With Microvessel Density in Pancreatic Ductal Adenocarcinoma, Recruits Monocytes, and Promotes Growth and Angiogenesis of Xenograft Tumors in Mice. Gastroenterology *154*, 675–688. https://doi.org/10.1053/j.gastro.2017.09.039.
57. Liu, C., Yao, Z., Wang, J., Zhang, W., Yang, Y., Zhang, Y., Qu, X., Zhu, Y., Zou, J., Peng, S., et al. (2020). Macrophage-derived CCL5 facilitates immune escape of colorectal cancer cells via the p65/STAT3-CSN5-PD-L1 pathway. Cell Death Differ. *27*, 1765–1781. https://doi.org/10.1038/s41418-019-0460-0.
58. Huang, R., Wang, S., Wang, N., Zheng, Y., Zhou, J., Yang, B., Wang, X., Zhang, J., Guo, L., Wang, S., et al. (2020). CCL5 derived from tumor-associated macrophages promotes prostate cancer stem cells and metastasis via activating beta-catenin/STAT3 signaling. Cell Death Dis. *11*, 234. https://doi.org/10.1038/s41419-020-2435-y.
59. Ding, H., Zhao, L., Dai, S., Li, L., Wang, F., and Shan, B. (2016). CCL5 secreted by tumor associated macrophages may be a new target in treatment of gastric cancer. Biomed. Pharmacother. *77*, 142–149. https://doi.org/10.1016/j.biopha.2015.12.004.
60. Yu-Ju Wu, C., Chen, C.H., Lin, C.Y., Feng, L.Y., Lin, Y.C., Wei, K.C., Huang, C.Y., Fang, J.Y., and Chen, P.Y. (2020). CCL5 of glioma-associated microglia/macrophages regulates glioma migration and invasion via calcium-dependent matrix metalloproteinase 2. Neuro Oncol. *22*, 253–266. https://doi.org/10.1093/neuonc/noz189.
61. Tajrishi, M.M., Zheng, T.S., Burkly, L.C., and Kumar, A. (2014). The TWEAK-Fn14 pathway: a potent regulator of skeletal muscle biology in health and disease. Cytokine Growth Factor Rev. *25*, 215–225. https://doi.org/10.1016/j.cytogfr.2013.12.004.
62. Sato, S., Ogura, Y., and Kumar, A. (2014). TWEAK/Fn14 Signaling Axis Mediates Skeletal Muscle Atrophy and Metabolic Dysfunction. Front. Immunol. *5*, 18. https://doi.org/10.3389/fimmu.2014.00018.
63. Meijboom, K.E., Sutton, E.R., McCallion, E., McFall, E., Anthony, D., Edwards, B., Kubinski, S., Tapken, I., Bünermann, I., Hazell, G., et al. (2022). Dysregulation of Tweak and Fn14 in skeletal muscle of spinal muscular atrophy mice. Skelet. Muscle *12*, 18. https://doi.org/10.1186/s13395-022-00301-z.
64. Bowerman, M., Salsac, C., Coque, E., Eiselt, É., Deschaumes, R.G., Brodovitch, A., Burkly, L.C., Scamps, F., and Raoul, C. (2015). Tweak regulates astrogliosis, microgliosis and skeletal muscle atrophy in a mouse model of amyotrophic lateral sclerosis. Hum. Mol. Genet. *24*, 3440–3456. https://doi.org/10.1093/hmg/ddv094.
65. Kumar, A., Bhatnagar, S., and Paul, P.K. (2012). TWEAK and TRAF6 regulate skeletal muscle atrophy. Curr. Opin. Clin. Nutr. Metab. Care *15*, 233–239. https://doi.org/10.1097/MCO.0b013e328351c3fc.
66. Dogra, C., Changotra, H., Wedhas, N., Qin, X., Wergedal, J.E., and Kumar, A. (2007). TNF-related weak inducer of apoptosis (TWEAK) is a potent skeletal muscle-wasting cytokine. FASEB J *21*, 1857–1869. https://doi.org/10.1096/fj.06-7537com.
67. Hénaut, L., Sanz, A.B., Martin-Sanchez, D., Carrasco, S., Villa-Bellosta, R., Aldamiz-Echevarria, G., Massy, Z.A., Sanchez-Nino, M.D., and Ortiz, A. (2016). TWEAK favors phosphate-induced calcification of vascular smooth muscle cells through canonical and non-canonical activation of NFkappaB. Cell Death Dis. *7*, e2305. https://doi.org/10.1038/cddis.2016.220.
68. Alvarez de Cienfuegos, A., Cheung, L.H., Mohamedali, K.A., Whitsett, T.G., Winkles, J.A., Hittelman, W.N., and Rosenblum, M.G. (2020). Therapeutic efficacy and safety of a human fusion construct targeting the TWEAK receptor Fn14 and containing a modified granzyme B. J. Immunother. Cancer *8*, e001138. https://doi.org/10.1136/jitc-2020-001138.
69. Lam, E.T., Eckhardt, S.G., Messersmith, W., Jimeno, A., O'Bryant, C.L., Ramanathan, R.K., Weiss, G.J., Chadha, M., Oey, A., Ding, H.T., et al. (2018). Phase I Study of Enavatuzumab, a First-in-Class Humanized Monoclonal Antibody Targeting the TWEAK Receptor, in Patients with Advanced Solid Tumors. Mol. Cancer Ther. *17*, 215–221. https://doi.org/10.1158/1535-7163.MCT-17-0330.
70. Noel, M., O'Reilly, E.M., Wolpin, B.M., Ryan, D.P., Bullock, A.J., Britten, C.D., Linehan, D.C., Belt, B.A., Gamelin, E.C., Ganguly, B., et al. (2020). Phase 1b study of a small molecule antagonist of human chemokine (C-C motif) receptor 2 (PF-04136309) in combination with nab-paclitaxel/gemcitabine in first-line treatment of metastatic pancreatic ductal adenocarcinoma. Invest. New Drugs *38*, 800–811. https://doi.org/10.1007/s10637-019-00830-3.
71. Öz, H.H., Cheng, E.C., Di Pietro, C., Tebaldi, T., Biancon, G., Zeiss, C., Zhang, P.X., Huang, P.H., Esquibies, S.S., Britto, C.J., et al. (2022). Recruited monocytes/macrophages drive pulmonary neutrophilic inflammation and irreversible lung tissue remodeling in cystic fibrosis. Cell Rep. *41*, 111797. https://doi.org/10.1016/j.celrep.2022.111797.
72. Tran, S., Baba, I., Poupel, L., Dussaud, S., Moreau, M., Gélineau, A., Marcelin, G., Magréau-Davy, E., Ouhachi, M., Lesnik, P., et al. (2020). Impaired Kupffer Cell Self-Renewal Alters the Liver Response to Lipid Overload during Non-alcoholic Steatohepatitis. Immunity *53*, 627–640.e5. https://doi.org/10.1016/j.immuni.2020.06.003.
73. Neehus, A.L., Carey, B., Landekic, M., Panikulam, P., Deutsch, G., Ogishi, M., Arango-Franco, C.A., Philippot, Q., Modaresi, M., Mohammadzadeh, I., et al. (2024). Human inherited CCR2 deficiency underlies progressive polycystic lung disease. Cell *187*, 390–408.e23. https://doi.org/10.1016/j.cell.2023.11.036.
74. Nywening, T.M., Belt, B.A., Cullinan, D.R., Panni, R.Z., Han, B.J., Sanford, D.E., Jacobs, R.C., Ye, J., Patel, A.A., Gillanders, W.E., et al. (2018). Targeting both tumour-associated CXCR2(+) neutrophils and CCR2(+)

macrophages disrupts myeloid recruitment and improves chemotherapeutic responses in pancreatic ductal adenocarcinoma. Gut *67*, 1112–1123. https://doi.org/10.1136/gutjnl-2017-313738.

75. Mitchem, J.B., Brennan, D.J., Knolhoff, B.L., Belt, B.A., Zhu, Y., Sanford, D.E., Belaygorod, L., Carpenter, D., Collins, L., Piwnica-Worms, D., et al. (2013). Targeting tumor-infiltrating macrophages decreases tumor-initiating cells, relieves immunosuppression, and improves chemotherapeutic responses. Cancer Res. *73*, 1128–1141. https://doi.org/10.1158/0008-5472.CAN-12-2731.
76. Dang, M.T., Gonzalez, M.V., Gaonkar, K.S., Rathi, K.S., Young, P., Arif, S., Zhai, L., Alam, Z., Devalaraja, S., To, T.K.J., et al. (2021). Macrophages in SHH subgroup medulloblastoma display dynamic heterogeneity that varies with treatment modality. Cell Rep. *34*, 108917. https://doi.org/10.1016/j.celrep.2021.108917.
77. Chen, Z., Soni, N., Pinero, G., Giotti, B., Eddins, D.J., Lindblad, K.E., Ross, J.L., Puigdelloses Vallcorba, M., Joshi, T., Angione, A., et al. (2023). Monocyte depletion enhances neutrophil influx and proneural to mesenchymal transition in glioblastoma. Nat. Commun. *14*, 1839. https://doi.org/10.1038/s41467-023-37361-8.
78. Sawanobori, Y., Ueha, S., Kurachi, M., Shimaoka, T., Talmadge, J.E., Abe, J., Shono, Y., Kitabatake, M., Kakimi, K., Mukaida, N., and Matsushima, K. (2008). Chemokine-mediated rapid turnover of myeloid-derived suppressor cells in tumor-bearing mice. Blood *111*, 5457–5466. https://doi.org/10.1182/blood-2008-01-136895.
79. Pham, K., Delitto, D., Knowlton, A.E., Hartlage, E.R., Madhavan, R., Gonzalo, D.H., Thomas, R.M., Behrns, K.E., George, T.J., Jr., Hughes, S.J., et al. (2016). Isolation of Pancreatic Cancer Cells from a Patient-Derived Xenograft Model Allows for Practical Expansion and Preserved Heterogeneity in Culture. Am. J. Pathol. *186*, 1537–1546. https://doi.org/10.1016/j.ajpath.2016.02.009.
80. Foley, K., Rucki, A.A., Xiao, Q., Zhou, D., Leubner, A., Mo, G., Kleponis, J., Wu, A.A., Sharma, R., Jiang, Q., et al. (2015). Semaphorin 3D autocrine signaling mediates the metastatic role of annexin A2 in pancreatic cancer. Sci. Signal. *8*, ra77. https://doi.org/10.1126/scisignal.aaa5823.
81. Zhou, Z., Zhang, J., Xu, C., Yang, J., Zhang, Y., Liu, M., Shi, X., Li, X., Zhan, H., Chen, W., et al. (2021). An integrated model of N6-methyladenosine regulators to predict tumor aggressiveness and immune evasion in pancreatic cancer. EBioMedicine *65*, 103271. https://doi.org/10.1016/j.ebiom.2021.103271.
82. Liu, M., Zhang, Y., Yang, J., Zhan, H., Zhou, Z., Jiang, Y., Shi, X., Fan, X., Zhang, J., Luo, W., et al. (2021). Zinc-dependent regulation of ZEB1 and YAP1 Coactivation promotes Epithelial-Mesenchymal transition Plasticity and metastasis in pancreatic cancer. Gastroenterology *160*, 1771–1783.e1771. https://doi.org/10.1053/j.gastro.2020.12.077.

STAR★METHODS

KEY RESOURCES TABLE

REAGENT or RESOURCE	SOURCE	IDENTIFIER
Antibodies		
mTWEAK	R&D systems	AF1237; RRID: AB_2206219
TWEAK	Abcam	Ab37170; RRID: AB_778691
Atrogin-1	ECM Biosciences	AP2041; RRID: AB_2246979
MuRF1	R&D systems	AF5366; RRID: AB_2208833
ZXDC	Proteintech	20530-1-AP; RRID: AB_10694823
TRAF6	Abcam	Ab40675; RRID: AB_778573
Phospho- NF-κB p65	Cell Signaling Technology	3033; RRID: AB_331284
NF-κB p65	Cell Signaling Technology	8242; RRID: AB_10859369
RELB	Cell Signaling Technology	10544; RRID: AB_2797727
Pan-CK	Cell Signaling Technology	4545; RRID: AB_490860
mCD68	Abcam	Ab53444; RRID: AB_869007
CD68	Invitrogen	14-0688-82; RRID: AB_11151139
FITC-Anti-CD45	Biolegend	157607; RRID: AB_2832554
PerCP Cy5.5 Anti-Ly-6G	Biolegend	127647; RRID: AB_2566318
APC-Cy7-Anti-F4/80	Biolegend	157315; RRID: AB_2894638
APC-Anti-CD86	Biolegend	105011; RRID: AB_493343
Brilliant-Anti-CD4	Biolegend	100559; RRID: AB_2562608
PE-Cy7-Anti-CD3	Biolegend	100219; RRID: AB_1732068
PE-*anti*-CD206 (MMR)	Biolegend	141705; RRID: AB_10896421
PE-Anti-CD8a	Bio-Rad	MCA609P647; RRID: AB_566916
PerCP-Anti-CD11b	Thermo Fisher	46-0112-80; RRID: AB_2866429
PE-Anti-CD192 (CCR2)	Biolegend	150609; RRID: AB_2616981
K63-Ub	Cell Signaling Technology	5621; RRID: AB_10827985
FLAG	MBL	M185-3L; RRID: AB_11123930
UBE2O	Cell Signaling Technology	83393; RRID: AB_2800015
mCCR5	R&D systems	MAB6138; RRID: AB_10717978
CCR5	R&D systems	MAB1802; RRID: AB_357919
CCL5	Cell Signaling Technology	36467
VCL	Proteintech	66305-1-Ig; RRID: AB_2810300
ACTB	Proteintech	66009-1-Ig; RRID: AB_2687938
GAPDH	Proteintech	60004-1-Ig; RRID: AB_2107436
Biological samples		
Primary tumor specimens and muscle samples	Johns Hopkins University	N/A
Chemicals, peptide, and recombinant proteins		
Recombinant mouse CCL2 protein	R&D systems	479-JE
Recombinant human CCL2/MCP1 protein	R&D systems	279-MC
Recombinant mouse CCL5/RANTES protein	R&D systems	478-MR
Recombinant human CCL5/RANTES protein	R&D systems	278-RN
Recombinant mouse TWEAK/TNFSF12 protein	R&D systems	1237-TW
Recombinant human TWEAK/TNFSF12 protein	R&D systems	1090-TW
Hygromycin B	Enzo Life Sciences	31282-04-9
Puromycin Dihydrochloride	Thermo Fisher Scientific	A1113803
ROCHE Complete™ Lysis-M	Millipore Sigma	04719956001

(*Continued on next page*)

Continued

REAGENT or RESOURCE	SOURCE	IDENTIFIER
Roche Protease inhibitors cOmplete™, Mini Protease Inhibitor Cocktail	Millipore Sigma	04693124001
Roche PhosSTOP™	Millipore Sigma	4906837001
Critical commercial assays		
Cytokine antibody array	Abcam	Ab193660
Pierce™ Magnetic ChIP Kit	Thermo Fisher Scientific	26157
BCA Protein Assay Kit	Thermo Fisher Scientific	23225
PureLink™ RNA Mini Kit	Thermo Fisher Scientific	12183018A
PureLink™ Quick Gel Extraction & PCR Purification Combo Kit	Thermo Fisher Scientific	K220001
Human TWEAK ELISA Kit	Thermo Fisher Scientific	EHTNFSF12
Mouse TWEAK ELISA Kit	Thermo Fisher Scientific	EMTNFSF12
Mouse RANTES ELISA Kit	Raybiotech	ELM-RANTES-1
Human CCL2/MCP1 ELISA Kit	Raybiotech	ELH-MCP1-1
Mouse CCL2/MCP1 ELISA kit	Raybiotech	ELM-MCP1-1
RANTES Mouse Instant ELISA™ Kit	Thermo Fisher Scientific	BMS6009INST
Experimental models: Cell lines		
KPC	Johns Hopkins University	N/A
AsPC-1	ATCC	CRL-1682
C2C12	ATCC	CRL-1772
THP-1	ATCC	TIB-202
RAW264.7	ATCC	TIB-71
PDX46	UTHealth	N/A
PDX87	UTHealth	N/A
Deposited data		
RNA-seq data from TCGA database	The Cancer Genome Atlas Program (TCGA)	https://portal.gdc.cancer.gov/
Single-cell transcriptomics analysis of pancreatic primary tumor and metastatic biopsy tissues	https://doi.org/10.1186/s13073-020-00776-9	GEO: GSE154778
Bulk RNA-seq data	https://doi.org/10.1038/s41467-022-32135-0	GEO: GSE165856
Software and algorithms		
FlowJo	TreeStar	https://www.flowjo.com/solutions/flowjo
IBM SPSS Statistics 20	IBM	https://www.ibm.com/products/spss-statistics
R v4.2.3	N/A	https://www.r-project.org/
ImageJ	NIH	https://imagej.nih.gov/ij/
Prism 10	GraphPad	https://www.graphpad.com

RESOURCE AVAILABILITY

Lead contact

Further information and requests for resources and reagents should be directed to and will be fulfilled by the Lead contact, Min Li (Min-Li@ouhsc.edu).

Materials availability

This study did not generate new unique reagents. Plasmids generated in this study are available from the lead contact with a completed Materials Transfer Agreement.

Data and code availability

Bulk RNA sequencing data are acquired from public databases. Accession links are available in the STAR methods. This study did not generate new unique codes. All codes are publicly available. Accession links are available in the key resources table. Any additional information required to reanalyze the data reported in this paper is available from the lead contact upon request.

EXPERIMENTAL MODEL AND SUBJECT DETAILS

Cell lines

AsPC-1 cells, RAW 264.7 cells, THP-1 and C2C12 myoblasts were purchased from American Type Culture Collection (ATCC, Rockville, MD). PDX46 and PDX87 cells are patient-derived primary human pancreatic cancer cells, which were established by Dr. Jose Trevino (Virginia Commonwealth University).[79] KPC cell line was kindly provided by Dr. Elizabeth Jaffee. The KPC cells were developed from *KRAS*^{G12D} *TP53*^{R172H} *PDX-1-CRE*$^{+/+}$ (KPC) mice which were backcrossed onto a C57BL/6 background for nine generations.[80] AsPC-1 cells were cultured in RPMI 1640 medium supplemented with 10% fetal bovine serum (FBS). KPC cells were cultured in RPMI 1640 medium with 10% FBS and 1% non-essential amino acids. THP-1 cells were cultured in RPMI 1640 medium with 10% FBS and 2-mercaptoethanol to a final concentration of 0.05 mM. PDX46 and PDX87 cells were culture in Dulbecco's Modified Eagle Medium F12 (DMEM-F12) with 10% FBS and 20 ng/mL EGF. C2C12 myoblasts and RAW 264.7 cells were cultured in DMEM medium with 10% FBS. Differentiation of C2C12 myoblasts was induced by 3% horse serum for 5 days to form myotubes. Conditioned medium collected from pancreatic cancer cells was then added to C2C12 myotubes to induce muscle atrophy.

Transgenic mouse models

C57BL/6 WT and *Ccr2*$^{-/-}$ mice (B6.129S4-Ccr2tm1Ifc/J. Strain #:004999) were obtained from The Jackson Laboratory. All mice were housed at the animal facility at University of Oklahoma Health Sciences Center (OUHSC). All animal experiments were approved by the Institutional Animal Care and Use Committee (IACUC) at OUHSC and were conducted in compliance with the National Institutes of Health (NIH) Guide for the animal studies. All mice were maintained under specific pathogen-free conditions in the animal facility.

Clinical samples

Human pancreatic cancer tissue and muscle tissue samples were obtained from Johns Hopkins University. This study was approved by the Institutional Review Board (IRB) at OUHSC. Banked de-identified tissues were used. Written consent from all subjects was obtained. Individuals with over 5% of body weight loss in the past 6 months were defined as having cachexia.[4] In this study, we defined ''less cachexia'' as those with less than 10% of body weight loss in the past 6 months. Those with more than 10% body weight loss in the past 6 months are considered as ''severe cachexia''. The prevalence of cancer cachexia and percentage of body weight loss were obtained from previous studies.[4]

METHOD DETAILS

Stable cell line construction

TWEAK overexpression stable cell lines were developed using the lentivirus vector from Genecopoeia following the manufacturer's instructions. The stable cell lines were selected by adding hygromycin (400 μg/mL) or puromycin (1.5 μg/mL) into the culture medium. Three individual lines were selected for each stable cell.

Chromatin immunoprecipitation assay

The chromatin immunoprecipitation (ChIP) assay was performed in KPC cells by using the anti-NF-κB p65 antibody with the Magnetic Chromatin Immunoprecipitation System (Life Technologies) following the manufacturer's protocol. After the antibody was pulled down, the target DNA fragment was amplified and determined by PCR. The sequences for mTWEAK ChIP assay are: Forward: 5′ CCTATGCTGGGAAGGAGGTAAT 3'; Reverse: 5′ CCTGGCCCCAGGAACTCA 3'.

Dual luciferase assay for promoter activity

The dual luciferase reporter plasmid containing the wild type promoter region of mouse TWEAK gene (NM_011614) was purchased from Genecopoeia (Cat# MPRM52541-PL01). The p65 potential binding sites were predicted using the JASPAR and PROMO tools. The three most potential binding sites for p65 were mutated using the QuikChange lightning multi-site-directed mutagenesis kit (Agilent Tech. Cat# 210515). The wild type or mutant promoter plasmids were co-transfected with sh-p65 plasmid into KPC cells using lipofectamine 3000 (ThermoFisher, L3000075) with the standard protocol. The mTWEAK promoter activities were acquired by the measuring the ratio of luminescence strength of firefly luciferase reporter with the renilla luciferase tracking gene, using the Dual-Luciferase Reporter Assay System (Promega, Cat# E1960) on Synergy H1 light Luminescence reader (BioTek Inc.).

The sequences of the potential binding site of p65 on the promoter region of mTWEAK are:
Site-1: GGGGAATTCT (−131 ∼ −140 bp); Site-2: TGCTTTCCCA (−1209–1211 bp); Site-3: TCTTTTCCCC (−1334 ∼ −1343 bp)
The sequences of mutagenesis primers for mTWEAK promoter are:
Site-1 mut primer: 5′ GCAGACTTGAAACAAGTTGGGGCCAAAACTGGAAGAGGGAA TCTCAACTC 3'; Site-2 mut primer: 5' TGCC TCTGTTTCCCAAGTGCTAAGGCACCTT TTATTACCCCACACC 3'; Site-3 mut primer: 5' CTGCTTGTAGTTGGTCTTTGCTGCT TTA TAGGTTCTAATGGCC ACTTTTATTTTTTCTTCTTC 3'

Western blot analysis

Cell lysate protein was isolated and loaded on SDS polyacrylamide gels as previously described.[4] Membranes were incubated with appropriate primary antibodies at 4°C overnight. After washing with 0.1% Tween 20-TBS, the membranes were incubated with an HRP secondary antibody for 2 h at room temperature. Immunoreactive bands were detected using an enhanced chemiluminescent (ECL) plus reagent kit.

Immunohistochemical staining

Human pancreatic cancer tumor tissue and muscle tissue, KPC GEMM tumor tissue, KPC orthotopic allograft tumor and muscle tissue were collected and fixed with formalin and embedded with paraffin and were sectioned into 4 μm slides. Slides were deparaffinized and incubated with 3% hydrogen peroxide solution to quench endogenous peroxidase activity for 15 min and then steamed for 15 min for the antigen retrieval and incubated in blocking buffer for 30 min at room temperature and incubated with antibody against TWEAK (Abcam, 1:100), CD68 (1:200) and were incubated overnight at 4°C. After washing with TBS, slides were incubated with polymer secondary antibody for 30 min (Vector Laboratories). Immune complexes were detected with diaminobenzidine (DAB) under a phase-contrast microscope. The sections were then dehydrated, mounted and observed under the microscope. Cross-sectional areas of muscle tissue (H&E staining) were quantified by ImageJ software.

ELISA assay

A total of 100 μL cell culture medium or serum as loaded onto the 96 well plate at 4°C overnight or 2.5 h at room temperature. Incubate with biotinylated antibody for 1 h and then washed 4 times with Wash Buffer. Incubate with Streptavidin-HRP solution for 45 min and then then washed 4 times with Wash Buffer. Add TMB One-Step Substrate Reagent on each well for 30 min and then add Stop solution. The absorbance was read at 450 nm and normalized at 620 nm.

In silico analysis

The Cancer Genome Atlas (TCGA) datasets were obtained from GDC data portal (https://portal.gdc.cancer.gov/). GEO datasets (GSE154778 and GSE165856) were obtained from Gene Expression Omnibus (https://www.ncbi.nlm.nih.gov/geo/). Percentages of immune cells were examined via CIBERSORTx platform (https://cibersortx.stanford.edu/). The analysis of TCGA data, GEO data and immune infiltration was performed as previously described.[81] Cancer cachexia prevalence and body weight loss of each cancer type were obtained from the literature.[4]

Pancreatic cancer allograft mouse models

Mouse models were constructed as previously described.[24,82] Briefly, KPC cell lines were harvested and resuspended in RPMI-1640 medium. A total of 3×10^5 KPC cells in 50 μL culture medium were injected into the pancreas of 6–7 weeks-old C57BL/6 WT or *Ccr2*$^{-/-}$ mice. The peritoneum and skin were closed with 4.0 surgical sutures. All mice were cared for in accordance with the Office for Protection from Research Risks (OPRR) and Animal Welfare Act Guidelines under an animal protocol approved by the Animal Welfare Committee at OUHSC. We sacrificed all the mice on the same day when the tumors of some mice were too large or some mice reached moribund. Tumor and muscle tissues were collected for further study.

QUANTIFICATION AND STATISTICAL ANALYSIS

All Statistical analyses were performed in Prism 10, IBM SPSS Statistics 20 and R (R version 4.2.3). Quantitative results are shown as mean ± SD. Overall difference among groups were assessed by ANOVA and post-hoc Dunnett's multiple comparison tests were used to compare data from control and each treated group. Two-group comparisons were analyzed by Student's t-tests. Mann-Whitney test was applied for the analysis of IHC staining of CD68 in clinical samples because the samples are unpaired and the data is not normally distributed. All tests were two-sided. Survival analysis was performed using Log rank test and the cut-off value was manually defined. p value < 0.05 was considered statistically significant.